Department of Electrical
and
Computer Systems Engineering

Technical Report
MECSE-5-2005

SIMULINK Models for Advanced Optical Communications: Part IV- DQPSK Modulation Format

L.N. Binh and B. Laville

MONASH
UNIVERSITY

SIMULINK MODELS FOR ADVANCED OPTICAL COMMUNICATIONS:

PART IV- DQPSK MODULATION FORMAT

LN Binh and B. Laville

Department of Electrical and Computer Systems Engineering, Monash University, Clayton, Melbourne, Victoria 3168, Australia. e-mail: le.nguyen.binh@eng.monash.edu.au

Abstract:

Given that the demands of ultra-wideband transmission over the Internet, transmission techniques are now considered to be very important. Either by deployment of new advanced fibres with ultra-high bit rate or upgrading current RZ- 10 Gb/s DWDM optical systems with 40 Gb/s channels interleaved or muxed with existing traffic infrastructure we can extend the capacity to Terabit/s with minimum upgrading tasks. Modulation formats are considered to be the most efficient technique to respond to current demands and moderately simple to implement in the photonic domain and offer 3-6 dB power gain as well as much more tolerable to linear and nonlinear dispersion impairments. Modulation formats such RZ-OOK , NRZ- OOK, CSRZ, CS-NRZ-OOK, RZ- and NRZ -DPSK, and the DQPSK can be employed for lightwave transmission. A number of these modulation formats have been reported [1, 2].

In this report we present Part IV of the series of the simulator based on Matlab™ Simulink for optically amplified transmission systems (SOATS). This part reports the DPQPSK transmission technique of single lightwave channel over optical fiber communication systems. It is capable of doubling the bit-rate compared to conventional OOK signaling techniques. The simulator has been developed extensively employing theblocksets of communication and signal processing of the Matla ™ Simulink. A high capacity 20 Gb/s (2 x 10Gb/s) and 40 Gb/s can be extended from 10 Gb/s channels.

The versatile nature of SOATS demonstrates the effects of mismatched dispersion management, hence dispersion penalty in fiber transmission links. Photonic components integrated in the model can be user-defined, enhanced or removed as desired. Essential theoretical background of the design of the optical DQPSK system is given. Detailed operation and purpose of each component model and its representation in Simulink

blocksets are described. Stages required for future extension of this simulator to support DWDM operation to allow Tb/s transmission with N x 40 Gb/s systems are also outlined.

TABLE OF CONTENTS

TABLE OF FIGURES

1 Introduction

The demand for increasing the transmission capacity of optical fiber transmission systems has prompted many researchers and companies to investigate cheaper, high bandwidth optical fiber system alternatives. A substantial amount of research has been pursued into developing high transmission rate systems which now extend into the terabit per second region[3]. A large proportion of these investigations have focused on the design of optical systems as a whole. By this we imply that many proposals made implement different performance improvement techniques such as the application of pre-transmission dispersion management, amplification and on some circumstances, investigate the benefits of utilizing different optical carrier sources[4]. An area of development which has had a great deal of research interest and applications is the dense wavelength division multiplexing (DWDM) optical fiber system. This system typically transmits multiple wavelengths on a single SM fiber. This method has been one of the key contributors to enhance the optical transmission channel capacity.

This report investigates the limitations of a single channel driven by the DQPSK signaling technique. Recently, interests have been shown towards the development of DQPSK transmission systems. These systems have been shown to be more tolerant to the effects of chromatic dispersion and other non-linear effects compared to conventional OOK[5]. The DQPSK technique also doubles the spectral efficiency (b/s/Hz) by encoding two bits of data per symbol in a differential phase shift format. The development and simulation of an optical DQPSK transmission link system using Matlab Simulink are described. The system is compared, to within certain limitations, with experimental results published papers [6]. We have, in particular, analyzed the impairments on system performance due to chromatic dispersion effects, self phase modulation (SPM), non-linear effects and receiver noise effects. In order to access these effects we have implemented these real performance degrading effects into the simulations based on theoretical knowledge. The flexible nature of the simulation platform offered by Simulink allows simulation ease for modern optical communication systems. Maintaining a focus on developing the single channel DQPSK system by simulating the effects of real optical devices in our laboratory, such as transmitter configuration, Mach Zehnder modulators, optical fiber (propagation models) etc allow for direct translation to experimental configurations.

The simulator developed here is integrated with other Simulink models to facilitate the simulation of all aspects of a 10 Gb/s DWDM system by incorporating certain simulation components (i.e. EDFA, Fiber models) to compare with those obtained experimentally. This report is organized as follows: Section 3 describes the backgrounds of theoretical development, Section 4 focuses on the DQPSK modulation format, Section 5 describes the simulator development using the Simulink platform of Matlab. This section also demonstrates the optical fiber communications Simulator for 20 Gb/s single channel DQPSK and finally Section 6 gives concluding remarks, the problems and future works.

2 Background

Before considering the details of the optical DQPSK transmitter design, we clarify the definitions, applications and theoretical background of optical components used in our model. The ITU-T standards (G.694.1) which have been recommended to ensure correct reliability and delivery of data are considered at a later stage. In this design we have assumed single channel transmission with an operating channel wavelength of 1550 nm. DWDM systems typically consist of many photonic components.

3 DWDM optical transmission system

Given the increase in demand for transmission capacity of modern optical fiber communication systems, considerations into alternative methods which allow for this increase need to be assessed. There exist two alternative options: (1) improves transmission bandwidth by merely *increasing the data rate*. Current transmitters used in some modern optical fiber systems operate at 40Gb/s. This approach can become quite costly when used in systems with several data sources (i.e video, data etc) (2) *increases the number of transmitters (wavelengths)* and thus the overall transmission rate by the same factor. Basically multiple wavelengths are transmitted on the one fiber. We consider for example, 20 channels operating at 10 Gb/s, each coupled in the one fiber making the overall transmission rate 200 Gb/s. With improving transmitter technology, DWDM systems employing 40Gb/s narrow spectral spaced channels have also allowed Tb/s transmission to become a reality. In this report we consider a single channel from the second alternative as the design of choice for the optical communication system, simulating a single channel from a DWDM system operating with 10 Gb/s per channel.

The foundations of the DWDM system rely on the ability to couple many wavelengths onto the one

transmission link. Using commercially available optical technology such as optical de/multiplexers, optical amplifiers and transmitter diodes, a point-to-point DWDM transmission system can be developed as shown below in *Figure 1*.

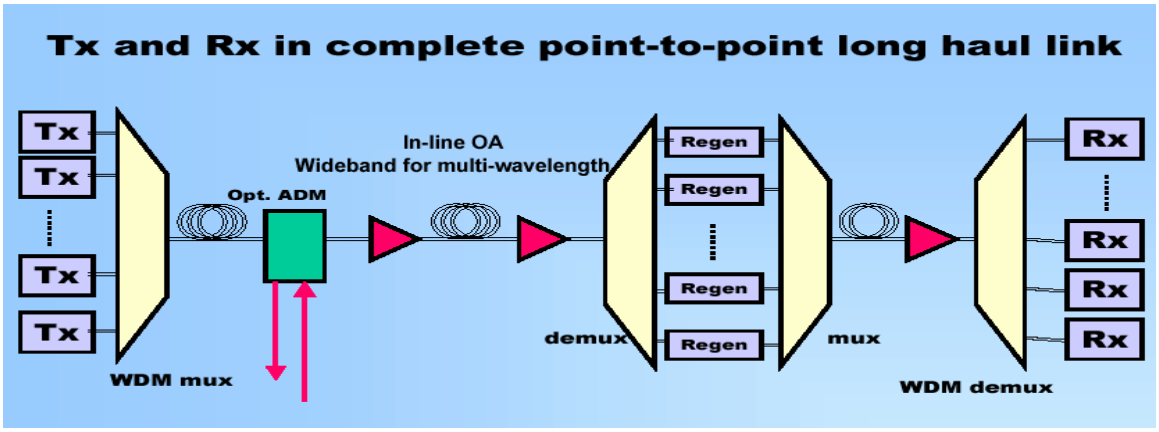

***Figure 1**: Typical architecture of DWDM transmission system*

For the purpose of this report project we simulate only one Peer to Peer transmission channel link to understand the fundamentals of the DQPSK signaling technique. Our simulation model consists of various optical devices with there behavior represented initially by theoretical interpretation. For example, in the transmitter, the optical components are placed in cascade which effectively modulates the optical carrier signal using a DQPSK format. The details of the transmitter configuration will be outlined later. It is important to note here that the principle behind DWDM is to associate each transmitter to a different data stream or effectively a different wavelength. Optical amplifiers, dispersion compensation modules and other optical devices may be added in between the fiber spans, this allows for long haul transmissions to be realized. These devices typically attempt to cancel any loss or attenuation in the signal as it propagates through the fiber.

The optical receivers (Rx) normally consisting of photodetectors and other optical hardware such as a Mach-Zehnder Delay interferometer (MZDI) in the case of DQPSK transmission systems and other differential encoding systems. These optical devices allow for the demodulation of the received signal and allow measurements of bit error rate (BER) and other system performance parameters to be evaluated using the eye diagram monitored by the scope at an appropriate point of the system.

DQPSK Transmitter

Using the concept of feedback, the DFB laser is capable of providing a reliable single-mode optical carrier [7]. It is constructed using a cavity enclosed on by both ends by a grating. Light is reflected internally in the cavity until the phase of an incident and reflected wave are matched. The light is then allowed to propagate. In this report we simulate the DFB laser diode using a signal generator.

Mach-Zehnder interferometric modulators (MZIM) are the most widely used as the photonic devices for external modulating the generated lightwaves. Although several types of MZIMs exist, in this report project we consider the well known lithium niobate ($LiNbO_3$) single electrode modulator based on its common use in 10G b/s PSK systems. Its role in most DWDM systems, and in this report project, is to externally modulate the carrier phase via the electro-optic effects and is thus usually placed in cascade with a DFB laser. The MZIM consists of a Y splitter (3dB), two waveguide arms and a Y combiner as shown in `Figure 2`.

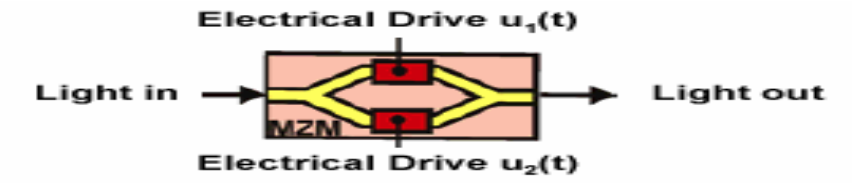

***Figure 2**: Mach Zehnder modulator[8]*

The electro-optic effect allows the refractive index of the material to change as a response to an applied voltages $u_2(t)$ *and* $u_1(t)$. For single electrode MZIM also known as the *modulating data stream* $u_1(t)$ *equals to zero.* The phase of the signal as it passes through this region of applied voltage (binary or sinusoidally varying) is changed. At the input, the power of the incident carrier is split equally, one carrier wave experiences a phase change (assumed 0 or π rad in this report), while the other passes through unchanged, two waves emerge and interfere with each other at the output. It should be noted that the optical carrier that has experienced the *0 or* π *phase shift* (in the lower arm of MZIM) is of great importance since the differential phase of this waveform will represent the first encoded bit of the two bits (di-bit) to be transmitted. A typical driving Voltage-to-Intensity transfer characteristic of the MZIM is shown in Figure 3. The MZIMs are biased at the minimum transmission point with biasing voltage, V_π (~3.5V in practice, with $2V_{\pi p\text{-}p}$ Non-Return to Zero driving voltage swing) and $V_\pi/2$ for the second MZIM (with $V_{\pi p\text{-}p}$ sinusoidal [approx RZ] driving voltage swing). Details of why we need two MZIMs are given later.

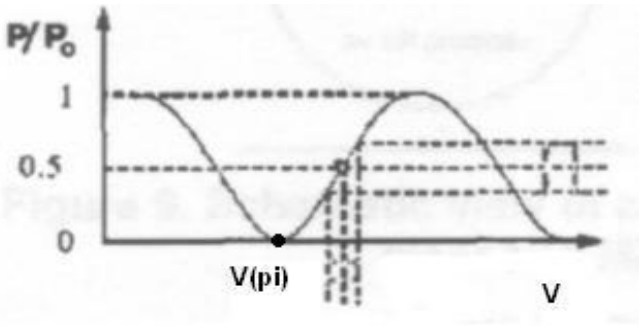

***Figure 3**: MZIM power (amplitude) versus voltage transfer characteristic[9]*

The MZIM is also a useful device in its response to certain high bit rate pulse shapes (e.g. NRZ, RZ) which can be used in replacement of a normal phase modulator (PM) biased to π phase shift. Other PMs simulated in this report operate under the same physical principles as the MZIM however are assumed to be biased to produce a π/2 phase shift in the optical carrier.

Optical Fibers

Note that in this report we only consider the linear model for lightwaves propagation in fiber[10]. Fibers allow digitized light signals to propagate without loss of signal for distances beyond 100 km spans with loss compensated by optical amplification[9]. Fiber technology has improved dramatically with attenuation levels reaching 0.25dB/km or better in the 1550 nm C-, L- and S-bands [11].

Chromatic dispersion is a property of optical fibers which limits the performance of the optical fiber communication system. Chromatic dispersion is the effect of pulse spreading or broadening and can reduce the integrity of a received signal unless appropriate dispersion compensation modules or fibers (DCM / DCF) are included in the system design. Two types of chromatic dispersion exists, firstly, *material dispersion* is caused by the fact that multiple wavelengths "see" different refractive indexes [12], the velocity of propagation in the fiber, given a wavelength dependent refractive index, is thus $c/n(\lambda)$. Secondly, effects of *waveguide dispersion* are heavily dependent on the geometrical characteristics of the fiber. Thus effectively there is a strong relationship between the relative refractive index and the normalized frequency parameter V[12]. Thus the bandwidth of an optically modulated signal influences the impairments due to propagation.

The polarization mode dispersion (PMD) is another important dispersion effect that introduces system power penalty. Although this parameter has only been observed experimentally[13], it can reduce the integrity of two adjacent pulses of transmitted data by introducing a third, unwanted pulse. PMD effects are integrated in another Simulink simulator.

The role of the chirp factor α, and in particular its influence on the performance of modern fiber optic systems is to be considered. Chirp, in particular transmitter chirp, is known to be a main contributor to spectral broadening[14], also limiting transmission to short distances (for $\alpha>0$)[1]. Thus to minimize the effects of chirp, we have considered the sources of this effect. In this report, as outlined later, we simulate the MZIM behavior. This electro-optic device is integral to the design of the DQPSK transmitter and is used in many DWDM systems. The MZIM is also available in the Monash University optics laboratory and is chosen as it provides superior signal integrity and normally has smaller chirping effects[16]. Frequency chirp is common in most optical transmitters and considered.

DQPSK Receiver

In this section we consider the operation and theory of the optical components that are integral to allowing for the demodulation and detection of the DQPSK transmitted signal.

The principle operation of this device is to convert phase-coded information, such as that generated by the DQPSK transmitter into an intensity signal which can be detected by a photodiode circuitry at the output of the delay interferometer (DI) arms. The intensity of the signal at the output of the DI arms is dependant on the phase difference between adjacent bits[15], $\Delta\phi_{\text{mod}}$ of the optical carrier in both the upper and lower arms, the relationship between phase and intensity is expressed as:

$$\mathrm{I}(\Delta\phi_{\text{mod}}) = 0.5\cos(\Delta\phi_{\text{mod}} \pm \frac{\pi}{4} + \delta\phi_{DI}) + 0.5 \quad (1)$$

where $\delta\phi_{DI}$ is a phase offset. *Figure 4* shows the optical device structure. Note that this is a Mach-Zehnder device and thus operates on the principles of interference between the two arms which is dependent on the phase difference. For the applications of DQPSK demodulation, the delay T is one bit in length (100ps for 10Gb/s operation) to allow for proper interference between

[1] for $\alpha<0$ (negative chirp) can actually increase the transmission distance by compressing the pulse, this technique is known as pre-chirp compensation.

two adjacent bits. Effectively the delayed signal acts as a phase reference for the incoming symbol. The extra phase delay (phase = $\pm\frac{\pi}{4}$) is normally implemented in practice for DQPSK systems only using integrated thermal heaters[20].

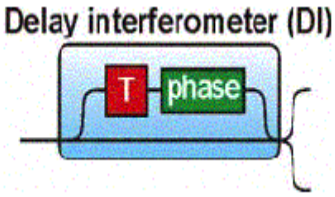

***Figure 4**: Delay interferometer[16]*

The phase to intensity characteristic of the MZDI is shown below in `Figure 5` along with the expected eye diagram that allows for performance measurements to be made.

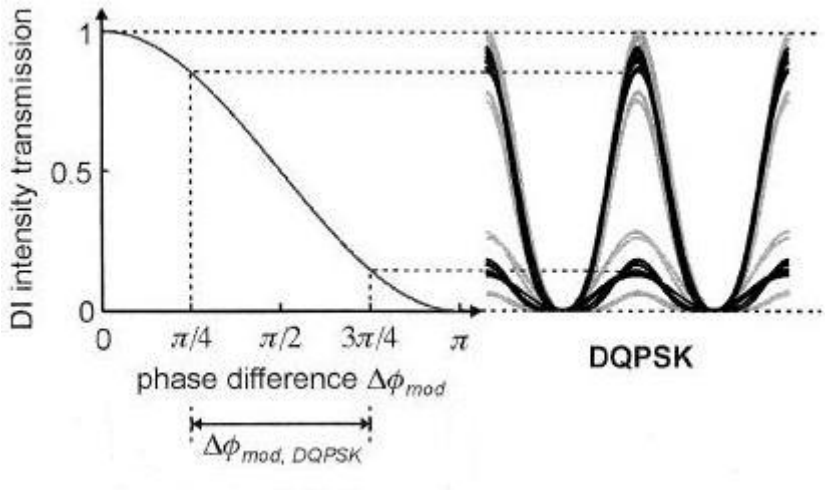

***Figure 5**: The phase to intensity characteristic of the MZDI and the expected eye diagram generated at the output of the MZDI based on the phase difference between the two arms, the lighter eye pattern is due to phase offset, $\delta\phi_{DI}$, from heater*

This optical eye diagram is then detected by a photodetector. These optical devices have shown to operate in a stable manner using either fiber-based or planar-lightwave-circuit (PLC) silica on silicon technologies. The current waveform shape at the output of the photodiode has been approximated by the *cos-like Ipulse* variable in our simulations.

In order to detect the optical intensity signal at the output of the MZDI shown in `Figure 6` and to display this signal for later Bit Error Rate (BER) analysis, a photodiode or a pair of balanced

photodiodes are required. The types most commonly used are the PIN and the avalanching photodiode (APD)[17]. The primary objective of the photodiode is to produce a conversion from optical photonic energy to and electrical (electron flow) current. In this report project we are considering the PIN photodetector type. In practice these PIN diodes (reversed-biased) are placed at the output arms of the MZDI. It is common practice to use either single or balanced diode detection at the receiver however in practice the balanced receiver configuration has shown higher sensitivity of 3 dB improvement for DQPSK and other PSK modulation formats[18]. In this report we consider the single diode detection model for simplicity, however we suggest that balanced detection be investigated at some stage in the future.

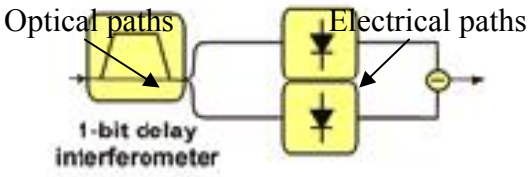

***Figure 6**: Balanced photodiode detection, diode placed at output of each MZDI arm.*

When a modulated signal of optical power *P(t)* falls on the detector, the primary photocurrent generated is given by[19]:

$$I_{sig} = \frac{\eta q P}{hf} = \Re P \tag{2}$$

where $\Re$ is the responsivity of the photodiode (A/W). A typical value of responsivity is 0.5 A/W.

Noise sources

In order to best simulate a true optical transmission systems we have considered various noise factors within the link, particularly at the receiver end. The noise sources implemented into the simulations include: the MZDI phase offset $\delta\phi_{DI}$, the photodiode noise effects (i.e. quantum shot noise, dark current and thermal noise) and the receiver amplifier equivalent noise at its input.

4 DQPSK modulation format and Simulink simulator

When digitizing data for transmission across many hundreds of kilometers many digital modulation formats have been proposed and investigated. This report investigates the DQPSK (Differential Quadrature Phase Shift Keying) modulation format. This modulation scheme although having been

in existence for quite some time had only been implemented in the electrical domain. Its application to optical systems proved difficult in the past as constant phase shifts of the optical carriers are to be maintained. However, with the improvement of optical technology and alternative transmitter design setup, these difficulties are eliminated.

One of the main attractive features of the DQPSK modulation format is that it offers both twice as much bandwidth and increased spectral efficiency compared to OOK. As an example, comparisons between 8 x 80Gb/s DQPSK systems and 8 x 40Gb/s OOK systems show that DQPSK modulation offers more superior performance (i.e. spectral efficiency)[5]. The very nature of the signaling process also allows non-coherent detection at a receiver to be possible, thus reducing the overall cost of the system design.

The DQPSK modulation format uses a differential form of phase shift modulation to the optical carrier which encodes the data. DQPSK is an extension to the simpler DPSK (Differential phase shift keying) format. Rather than having two possible symbol phase states (0 or π phase shift) between adjacent symbols, DQPSK is a four-symbol equivalent {0, π/2, π or 3π/2}. Depending on the desired di-bit combination to be encoded, the difference in phase, $\Delta\phi_{\text{mod}}$, between the two adjacent symbols (optical carrier pulses) is varied systematically. *Table 1* outlines this behavior.

Di-bit	**Phase difference $\Delta\phi = \phi_2 - \phi_1$ (degrees)**
00	0
01	90
10	180
11	270

***Table 1**: DQPSK modulation phase shifts*

Where ϕ_1 and ϕ_2 are the phase of adjacent symbols. The above table can also be represented in the form commonly known as a "constellation diagram" (see *Figure 7*). This graphically explains the signals state in both amplitude and phase.

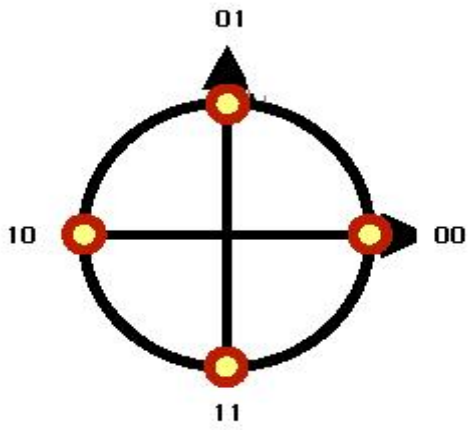

***Figure 7**: DQPSK signal constellation*

Ideally the amplitude should remain constant and the phase of the signal is changed during transitions, however due to the characteristics of the optical equipment (i.e. MZIM) some form of optical intensity modulation should in practice also be observed. This is usually termed as the patterning effect. This effect is investigated, however not implemented in the final simulator due to data pulse representation inaccuracies.

4.1 SIMULINK Simulator

4.1.1 Digital pulse shape and sampling

Given this report has been implemented in the Matlab subsidiary program Simulink, most of the data supported by the blocksets can only support discrete data sources/ values. Thus a means of converting continuous waveforms to discrete values is required. Signaling theory states that a continuous signal *s(t)* can be represented by a set of samples taken at a sampling frequency *(f_s)[20]*. This sampling frequency must be at least twice that of the highest frequency contained in the signal waveform, B. This is represented mathematically by:

$$f_s \geq 2B \text{ samples /second} \tag{3}$$

The value $f_s = 2B$ is referred to as the Nyquist rate. All samples made during the simulation are made at the Nyquist rate to ensure synchronization between data samples and to minimize sampling errors.

As mentioned earlier the concept of pulse shapes in applications to the MZIM. We consider now the return-to-zero (RZ) digital signal, the pulse shape used in the final design of this report. This

pulse shape has a duration of half the period (*T/2*), thus has a 50% duty cycle. In most modern optical systems, this RZ pulse shape is often approximated by a sinusoid having frequency 1/T Hz[21]. The brief nature of the pulse, makes the RZ pulse shape more tolerable to intersymbol interference (ISI) compared to the non-return-to-zero (NRZ) pulse shape however its power spectra occupies a larger bandwidth. In this report we consider the RZ pulse shape as it is more compatible with the simulation development. The NRZ pulse shape also has a data rate of *1/T* b/s however its duration is now T seconds. The power spectrum is also reduced to half that of the RZ pulse spectrum.

4.1.2 The simulator models

With adequate knowledge and theory of the optical components required in the design of a single channel 10 Gb/s DQPSK transmission link we can now consider the development process of the optical simulator. This simulator considers only one channel implementing the differential quadrature phase shift keying (DQPSK) signaling technique (total 20 Gb/s data rate); multiple channel configurations (DWDM) have been considered as future work. The primary design of a single channel operating efficiently was considered critical. We have developed this simulator package in three main steps, each relating to the three main components in the transmission link. These include the transmitter, fiber and receiver models. As this report focuses on the optical signaling technique DQPSK ever attempted in Matlab Simulink, especially how this signaling technique can be implemented in the optical domain using photonic hardware is essential. The work done uses a previously developed Simulink simulator[22] for implementing the OOK format as a guide.

The transmitter performing the DQPSK transmission format is developed first. This digital signaling technique can be implemented several ways using different hardwares. The final technique chosen proved to be the simplest to design and simulate using conventional data processing blocks in Simulink. The configuration of this transmission system is also partially based on the published works on DQPSK signaling transmission[5]. *Figure 8* shows the top level of the single channel optical DQPSK Simulink model developed. This model can be later altered and new blocks added to optimize the system to individual requirements.

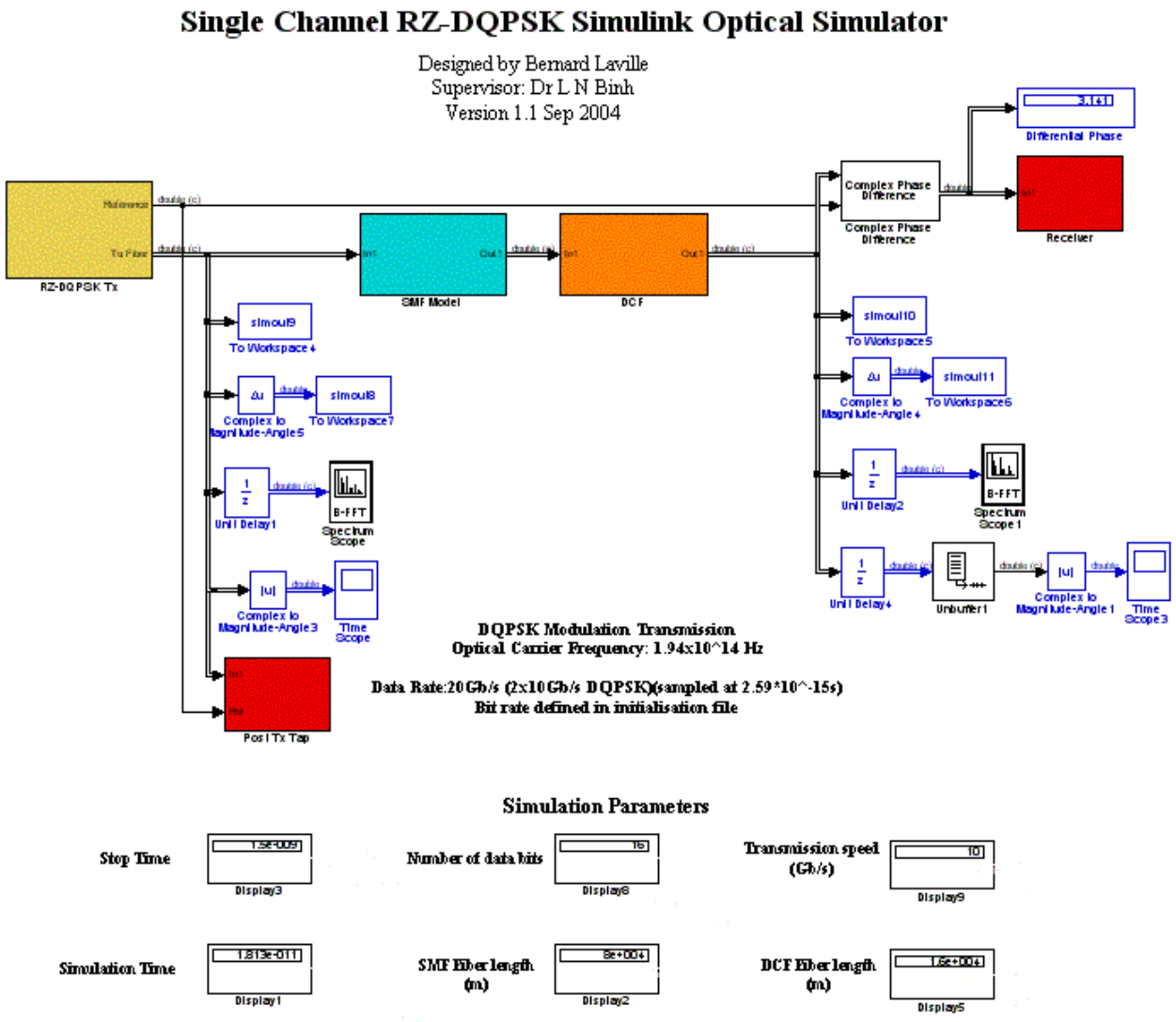

Figure 8 *RZ-DQPSK transmission Simulink optical simulator for single channel transmission*

The final results displayed during simulations include the *di-bit* NRZ electrical bit stream (2 x 10Gb/s) which modulates the optical carrier via the MZIM and PM, the spectrum of the transmitted optical carrier, the RZ time-domain pulse generated and finally the eye diagrams both before to fiber propagation and after to allow for BER testing and other system performance measurements. We now consider each block shown in *Figure 8* and present the development process.

4.2 Simulator Initialization

In order to commence the simulation of the RZ-DQPSK optical fiber communication system, variables used throughout the model need to be declared and defined. These variables include system parameters such as bit-rate, number of transmitted di-bits and fiber length and also allow for the automatic opening of the simulator model '*SingChanDQPSK_sim.mdl*'. These parameters are declared in a Matlab m-file named '*initialise_optical_simulator_DQPSK.m'*. This file must be executed before simulations can begin. It also presents the opportunity to change system parameters without having to find the location of the variable in the Simulink model. The m-file must be run again before new parameter values taking effective effect.

4.2.1 Assumptions

Simulink provides the user with the ability to simulate communications systems without the need of having a strong background in Matlab coding. An important requirement for the use of this program (Simulink) in modeling fiber optic systems is that the: **Simulink DSP blockset and Simulink Communications Blockset** are required. Without these blocksets certain features of the system can become very difficult to model.

To simplify some aspects of the transmitter design we have assumed that there are no chirping effects from the DFB laser, an ideal signal generator is used to represent the fixed wavelength light waves. This can be implemented using an X-cut $LiNbO_3$ MZIM. We have also assumed that there are no insertion losses (coupling losses), traveling losses or recombination losses for the MZIM. The optical intensity characteristic of the MZIM is assumed to be ideal, thus has a large extinction ratio (large dB difference between P_{max} and P_{min}). The minimum output power, P_{min}, of the MZIM is thus modeled mathematically to be zero at the minimum transmission point. Otherwise patterning effects would be observed on the eye diagram. We will report this patterning effect in another article.

4.2.2 Transmitter model

The transmitter is an integral component in any optical fiber communications system and thus we have given the transmitter design first priority in our simulations. Given that we have understood the operations of several key optical devices, we can specify the DQPSK transmitter model. The transmitter design is based on a design previously tested experimentally [5]. First we implement a

RZ pulse carving MZIM which generates the RZ pulse shape desired. Next an MZIM (generating 0 or π phase shift of OC) is to be coupled along with a Phase modulator (PM) which induces a 0 or π/2 phase shift of the optical carrier. When placed in this configuration the four phase states of the OC required by the DQPSK modulation format, *{0, π/2, π or 3π/2}*, can be achieved. Both the MZIM and PM are to be driven by random binary generators operating at 10 Gb/s. *Figure 9* shows the schematic diagram of the system transmitters for the RZ-DQPSK modulation. We originally started with the NRZ-DQPSK design however the RZ format is used more readily in practice and has proven to be more robust to system non-linearities[30]. ***Figure 10*** shows the Simulink model of the transmitter.

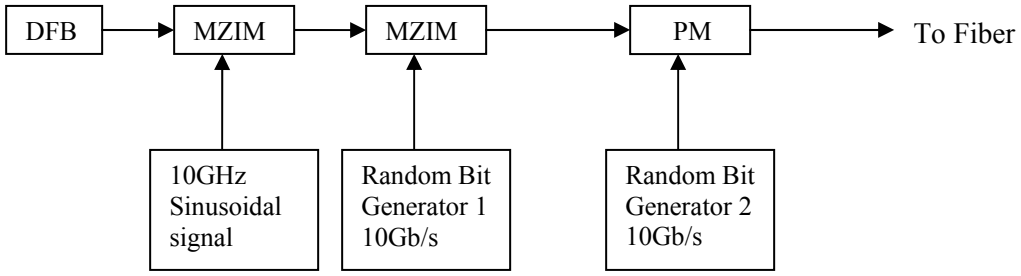

Figure 9*: Schematic of a channel implementing RZ-DQPSK modulation.*

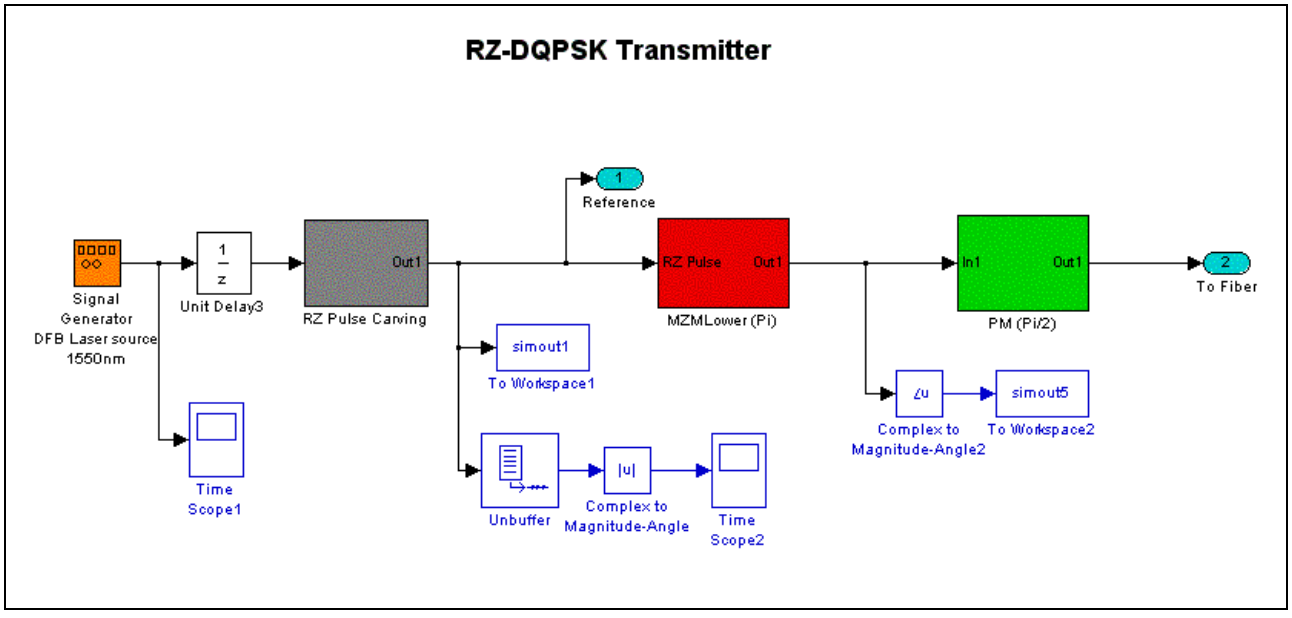

Figure 10: Simulink model of Figure 9, the unit delay block samples the continuous Signal generator waveform at Nyquist rate.

4.2.3 Optical carrier source model

As mentioned earlier, to simplify this part of the simulation development we are considering an ideal laser source (i.e. no frequency chirp present) and implement this in Simulink by selecting the *"Signal Generator"* block, represented by the block shown in Figure 11.

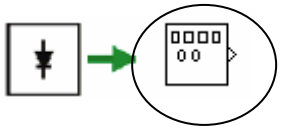

Figure 11: Signal Generator block in Simulink

This block models the desired sinusoidal optical carrier obtained from an ideal DFB laser which takes the mathematical form:

$$c(t) = A\cos(\omega_n t + \phi) \tag{4}$$

where ω_n and ϕ are the frequency and phase of the optical carrier respectively, with $\omega_n = 2\pi$ x 1.93 x 10^{14} rad/s corresponding to the 1550 nm operating wavelength. A, the amplitude of the optical carrier has been normalized for simplicity and is thus set to unity.

Due to the discrete nature in which Matlab stores and processes data, we need to sample this waveform and other signals to ensure synchronization, at certain intervals, T, in order to process the data through the system correctly. The *sample time* fields of some blocks are required, the Nyquist sampling time is inserted here. This technique maintains the integrity of the signals. According to the Nyquist theorem, this sampling interval is at least twice the highest frequency in the system. Thus:

$$\begin{aligned} & f_{sampling} \geq 2B \\ & \therefore T_{sampling} \leq \frac{1}{2B} s = 2.59 \times 10^{-15} s \end{aligned} \tag{5}$$

RZ pulse carving

The DQPSK transmitter performs a RZ pulse carving operation of the optical carrier lightwaves. This technique uses a sinusoidal driving voltage (10 GHz signal used as approximation to RZ pulse

shape for 10 Gb/s system to drive the MZIM. This driving signal, a 10 GHz sinusoid is modeled here by

$$u_{2RZ\text{-}MZIM}(t) = \frac{1}{2} + \frac{1}{2}\sin \omega t \,. \tag{6}$$

When multiplied by π gives a value between *0 and* π. This value is used to implement the required phase shifting of the optical carrier (in the lower arm) resulting in a pulse waveform that oscillates between maxima and minima with 63% duty cycle as shown in **Figure 12**. In this case the MZIM has a *biasing of* $V_\pi/2$ as shown in ***Figure 13***. *Figure 14* illustrates the Simulink model for the RZ pulse carving operation.

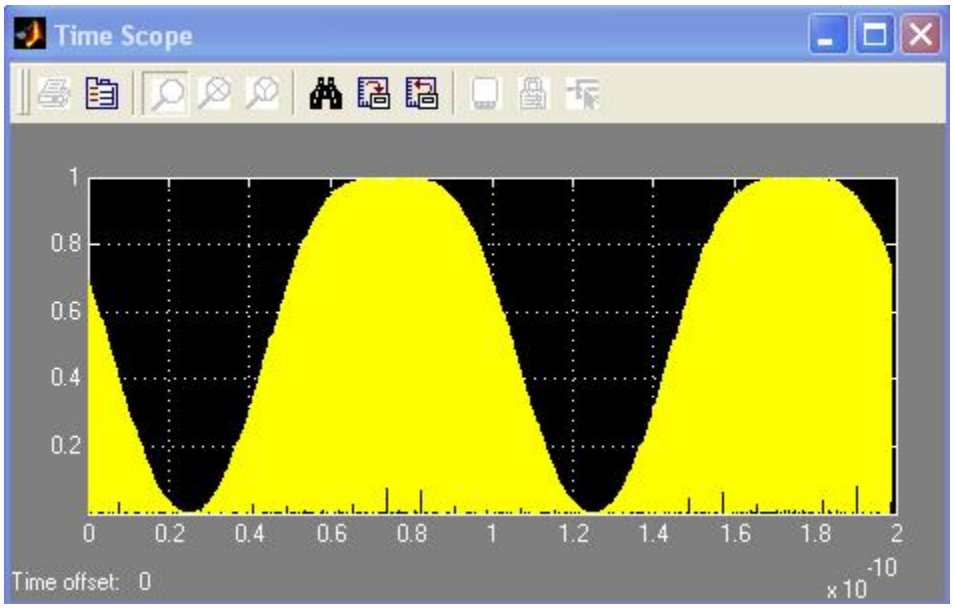

Figure 12*: The Optical carrier after RZ pulse carving using an MZIM driven by a 10 GHz electrical signal*

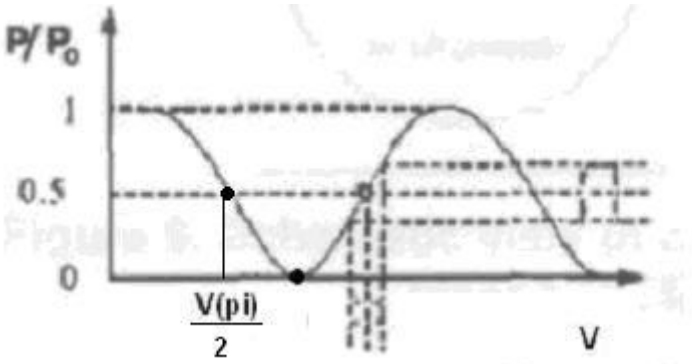

Figure 13: Biasing points of MZIM used for RZ pulse carving (shaping), carrier suppression if biased at the minimum transmission point (V_{pi}) or maximum transmission point if carving not required.

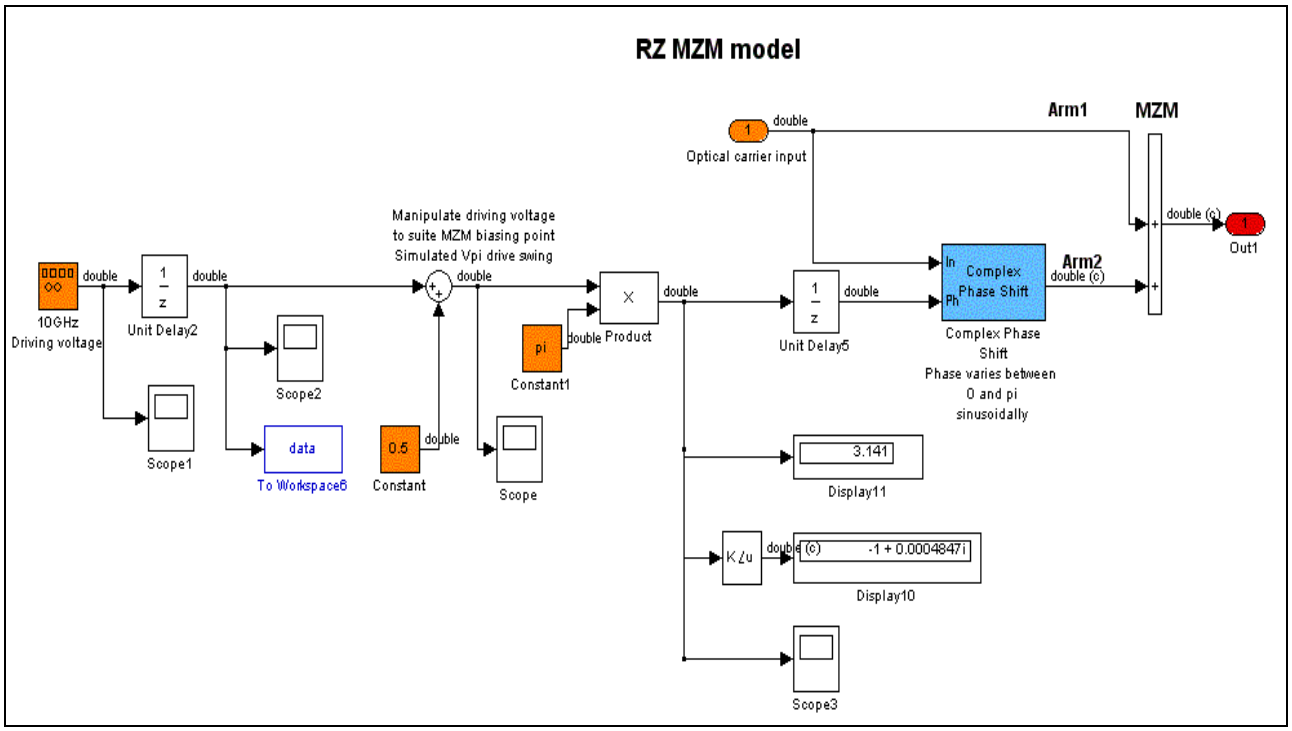

***Figure 14**: The Simulink RZ MZIM model*

The MZIM driving signal given by (8) is constructed using a 10 GHz signal of magnitude 0.5, we add 0.5 and multiply these values by π. The values injected to the 'Complex Phase Shift' block 'Ph' input has value between 0 and pi as described earlier. This block then phase shifts the optical carrier at the 'In' port by the amount of 'Ph'. This signal is then added to an unaltered optical

carrier simulating the Y recombiner of the MZIM. The signal shown in *Figure 14* is then passed to the second MZIM and the PM for phase modulation.

MZIM and PM models

In DQPSK transmission the second MZIM is commonly used as a 0 or π phase shifting device when biased at the minimum transmission point. Ideally a PM modulator, biased to produce a π phase shift would be used however these are expensive and do not operate well at high bit rates in practice. Thus as a substitute the MZIM, which is very responsive to 10 or even 40 Gb/s systems is used in practice and thus used in our simulations. The splitting of the optical carrier at the input of the MZIM thus causes the output, when viewed experimentally, to consist of two optical waveforms beating together, provided there has been some phase change in the lower arm. Thus in reality, it is the optical signal from the lower arm that is of greater importance as it has been phase shifted by $u_2(t)$ (refer *Figure 2*). Although the sinusoidal carrier has been reduced by 3 dB due to splitter, we assume for simplicity that it retains its initial input power. Thus in this report we only model the signal propagation through the lower arm of the MZIM, that is, the carrier will only experience either a 0 or π phase shift depending on the value of the digital driving voltage signal ('0' or '1' from Bernoulli block, refer to *Figure 15*).

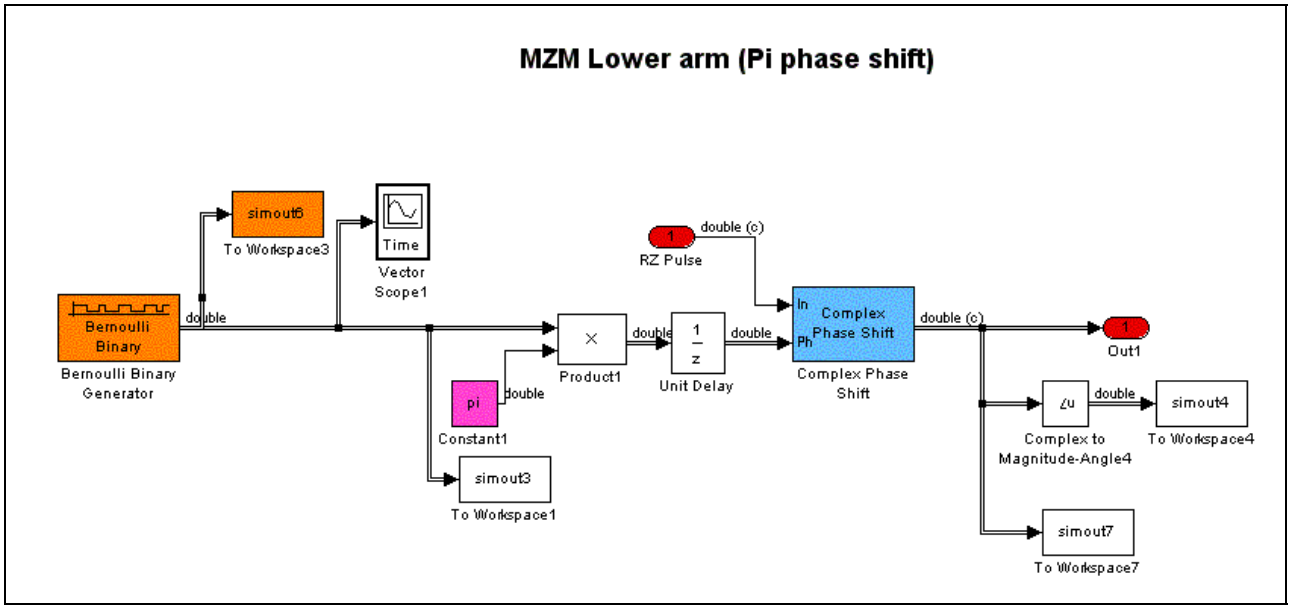

***Figure 15**: The MZIM simulation model- note the generation of either a 0 or π phase shift of the optical carrier.*

The 'Bernoulli Binary' block generates a NRZ random bit pattern which when multiplied by *pi* generates a value of either *{0,π}*. This value is sampled every bit period (via unit delay block every 100ps for 10Gb/s operation) and the RZ-pulse carved optical carrier is phase shifted by *0 or π* accordingly.

The Phase Modulator (PM) of the optical simulator operates on the same principles as the MZIM model, multiplying the random NRZ bit-stream by *π/2* instead of *π*. We also consider a different bit stream to that driving the MZIM. As can be seen in *Figure 16*, there is an extra 'unit delay block' at the output of the Bernoulli Binary generator, effectively delaying the original bit stream *by one bit period*. This ensures that the data driving the PM is 'uncorrelated' from the data driving the MZIM and that all four phase states of the signal constellation is achieved at some stage during simulation run-time.

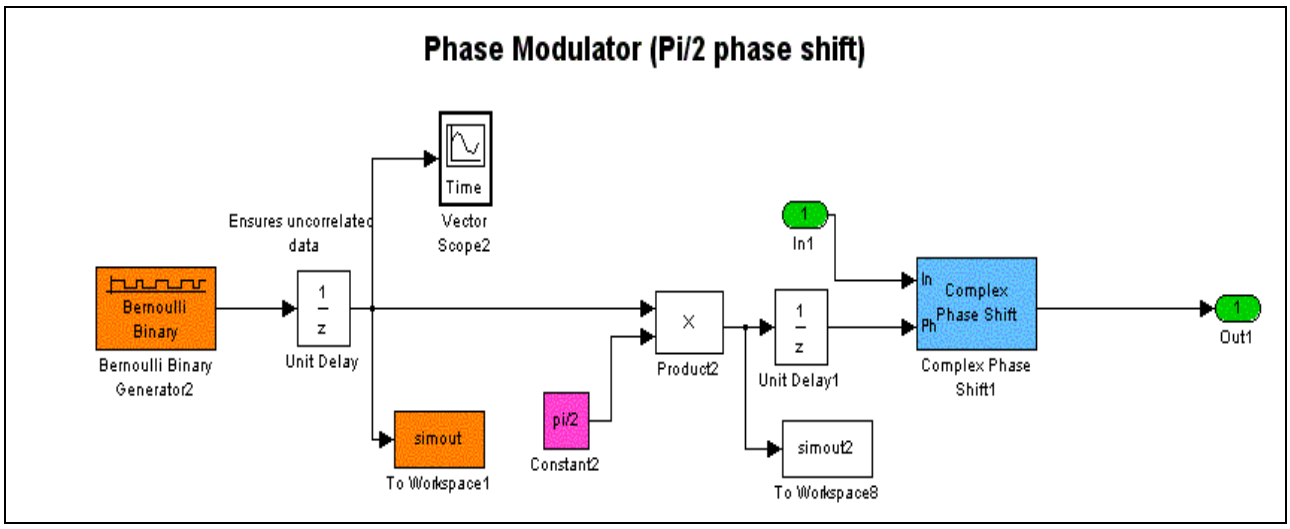

***Figure 16**: PM simulation model - the implementation of either a 0 or π/2 phase shift in the optical carrier.*

In practice the characteristic of uncorrelated data is achieved by the physical time delay due to signal propagation between the second MZIM and the PM or using complementary data streams[5].

As shown in ***Figure 10***, when the RZ pulse carver MZIM, an MZIM and PM driven by NRZ electrical signals are placed in cascade they modulate the optical carrier according to the DQPSK modulation format as required.

4.2.4 Linear fiber propagation model

Since the single channel RZ-DQPSK transmitter has been modeled, one can focus on the simulations of the signal propagation via the optical fiber. There have been several fiber models which have been proposed. An example of these proposals includes the 'Fiber split step model'[23] which models the linear and non-linear phenomena in the fiber as the two optical temporal lenses and a nonlinear operator in the frequency domain. Our developed model achieves this propagation accuracy by implementing fiber dispersion effects using time-domain digital signal processing and filtering technique that has been proven to be efficient in it computational resources. The split step model has been implemented in a report[22] and thus we consider an alternative fiber propagation model which considers the effects of dispersion on the system performance. Dispersion management in high capacity (>10Gb/s) optical networks is of great importance, thus we consider predominantly the effects of dispersion in this model and later analyze the effects of different dispersion management techniques by inserting dispersion compensation fibers of varying dispersion factors (ps/nm.km). We also consider the effects of fiber attenuation with values based on standard attenuation levels of modern day single mode optical fibers (Corning SMF-28).

This fiber model assumes that the SMF can be represented as a bandpass filter. The flat amplitude response in the passband was initially presented in the literature however as an extension we have considered the effects of attenuation to simulate true fiber propagation. The final mathematical representation of the fiber is derived by first considering the slope of the group delay whose dependence on the chromatic dispersion is given by[24]:

$$\frac{d\tau}{d\nu} = \frac{d\tau}{d\lambda}\frac{d\lambda}{d\nu} = \left(\frac{-1}{L}\frac{d\tau}{d\lambda}\right)\left(\frac{\lambda^2}{c}\right)L$$
$$where \quad \frac{-1}{L}\frac{d\tau}{d\lambda} = D(\lambda) \tag{7}$$

In (9), L is the fiber length, λ the operating wavelength, ν the optical frequency and *c* the speed of light. From these equations it can be shown that the equivalent model for the single mode fiber is expressed by the transfer function:

$$H(f) = e^{-j\pi D(\lambda)\frac{\lambda^2}{c}Lf^2} = e^{-j\pi D(\lambda)Lc} = e^{-j\pi D(\lambda)\lambda Lf} \tag{8}$$[34]

Since (8) is in the form of a frequency domain transfer function, it is more convenient to operate in the frequency domain as apposed to taking the convolution in the time domain. Determining the output of the fiber $\hat{X}_{out}(f)$ given an input modulated signal $\hat{X}_{in}(f)$ (where the ^ symbol refers to the Fast Fourier Transform (FFT) of x_{in} and x_{out}) is found by:

$$\hat{X}_{out}(f) = H(f).\hat{X}_{in}(f) \tag{9}$$

(8) is represented in block diagram as below in *Figure 17*.

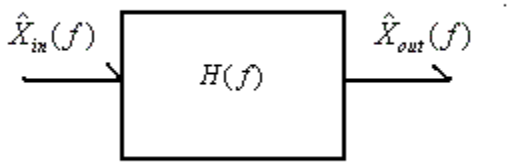

Figure 17: Block diagram of the linear fiber model, a low pass optical filter.

Thus by taking the FFT of the input modulated signal in Simulink then multiplying by *H(f)* and finally taking the IFFT (inverse FFT) we can accurately represent fiber propagation with any additional chromatic dispersion, thus making the model linear. For the standard SMF fiber model we use $D(\lambda)_{SMF}$ = *+17 ps/nm.km at 1550 nm wavelength*, L = 80km) with no optical amplifiers and for the dispersion compensation fiber (DCF) model we assume smaller length where, $D(\lambda)_{DCF}$ = *-85 ps/nm.km, L = 16 km*. This value of dispersion for the DCF cancels the dispersion effects of the SSMF and ensures that there is no or little loss of signal phase integrity at the receiver end. Given the Corning fiber SMF-28 manufacturers specifications quote an attenuation level of 0.2 dB/km, this implies a total of 16dB attenuation of optical power after 80km. This results in a power attenuation (Simulink gain block) of 0.03. This value is taken into account in the simulations as shown in *Figure 18* of the SMF Simulink model via the Gain block at the top of the model. Other fiber models are identically the same with modifications to the parameter values made as desired for dispersion compensation or the like. It is possible to change the fiber parameters in the model directly however it is suggested that the parameters be changed in the initialization file mentioned in 5.1 and the simulations run again with the new changes.

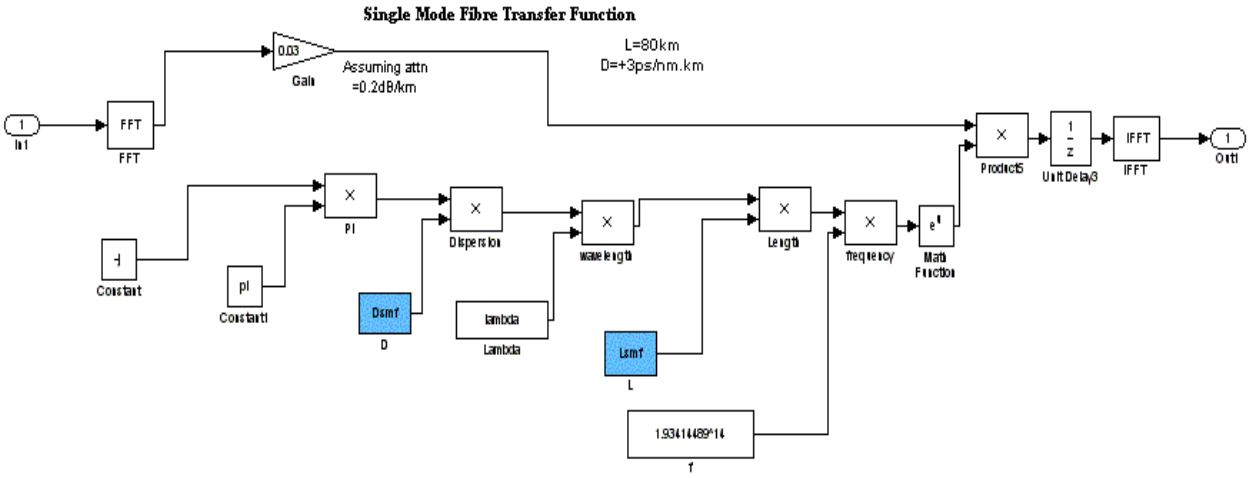

Figure 18 *SSMF Simulink model based on the LPF with 0.03 gain factor. Note the FFT and IFFT blocks*

It should be noted that no fiber non-linearities have been included in this fiber model. Due to time restrictions the fiber model is considered to be adequate for the needs of propagation modeling along with the effects of dispersion. It is suggested that the non-linear effects be considered for future work where effects such as self phase modulation (SPM) need to be considered. In this context we would need to consider the non-linear parameter γ, where γ is given by[25]:

$$\gamma = \frac{2\pi \bar{n}_2}{\lambda A_{eff}} \tag{10}$$

where A_{eff} is the core effective area of the fiber and is given by $2\pi r_o^2$ where r_o is the fiber spot size. The parameter $\bar{n}_2$ is known as the material non-linear refractive index and takes the value $2\text{x}10^{-20}$ m^2/W. This nonlinear factor is thus known to produce a nonlinear phase shift which is dependant on the input power P_{in} by[6]:

$$\phi_{NL} = \gamma P_{in} L_{eff} \tag{11}$$

where L_{eff} is the effective length of the fiber. To remain in a linear region of fiber propagation and minimizing the effects of SPM it is recommended that $\phi_{NL} << 1$[6]. In addition to the fiber model developed in *Figure 18* an additional non-linear phase ϕ_{NL} can be added (in the form $e^{-j\pi D(\lambda)\lambda L f + \phi_{NL}}$) in the case where $\phi_{NL} > 0.1$ say. A test of the value of ϕ_{NL}, which is dependant on the input power P_{in}

as shown in (13) can be performed and added into the model based on the results of the test. With this addition, the effects of SPM on system performance could be assessed.

4.2.5 Receiver model

Based on the physical setup used in practice, this model of the DQPSK receiver attempts to simulate, to within Simulink capabilities, some of the key principles allowing for the successful decoding of the DQPSK modulated signal. We also place an exact receiver model (block: Post Tx tap) before fiber propagation to allow for comparisons between pre and post fiber effects in eye diagram form. The scheme below is found to be regularly used for the modulation scheme mentioned previously in the transmitter component of this report. Note that due to the differential nature of the modulation process, the demodulation and detection stage can be considered as a 'non coherent' or 'Direct Detection' scheme. The absence of a local oscillator (LO) and any other extra photonic hardware (i.e. mixers etc) required in conventional detectors makes this demodulation technique attractive. Indeed this detection process is the self-homodyne detection scheme.

The receiver configuration used in this report is capable of demodulating the signal transmitted along the 96 km dispersion compensated fiber span. Since the modulation format used in this report typically encodes two bits of data per symbol it is necessary to extract both bits (termed 'real' and 'imaginary' bits[5]) from the one received symbol. The receiver configuration is as shown below in *Figure 19*.

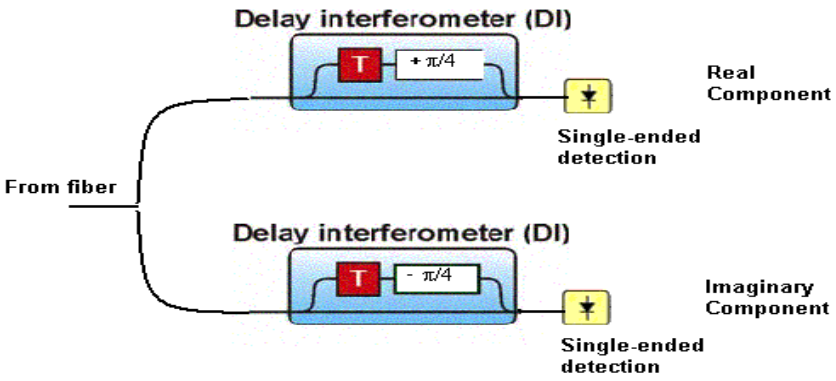

***Figure 19**: DQPSK receiver configuration using non-coherent direct detection- a self-homodyne technique.*

We now outline the purpose of the ± π/4 additional phase shift of the optical carrier implemented in the MZDI found in the receiver. Since the two bits to be encoded at the Tx are implemented via an

MZIM (0 or π phase shift) and the second bit is encoded via the PM (0 or π/2 phase shift) the two devices are said to be in 'quadrature' to one another. This implies that there is a π/2 phase difference between all signaling phase states, refer *Figure 7*. The additional + π/4 and - π/4 give a total π/2 phase difference between the upper and lower receiver branches shown in ***Figure 20***. Thus if data recovery was a main issue we could compare the real and imaginary bits received to those transmitted. However in this report we only consider the 'real component' received signal and asses the overall performance of the system via eye diagram analysis (using Q-factor method and BER).

In practice demodulation of the DQPSK signal uses the two branch configuration in *Figure 19* has been successful[18]. A balanced detection set up has proven to be more sensitive and 3 dB improvement as compared with one photodiode detection scheme. We present here the detection using a single photodetector. Balanced receiving system will be simulated in future work and the performance of sensitivity and BER is compared to the results obtained in this report. Thus the receiver model developed in Simulink is as shown below in ***Figure 20***.

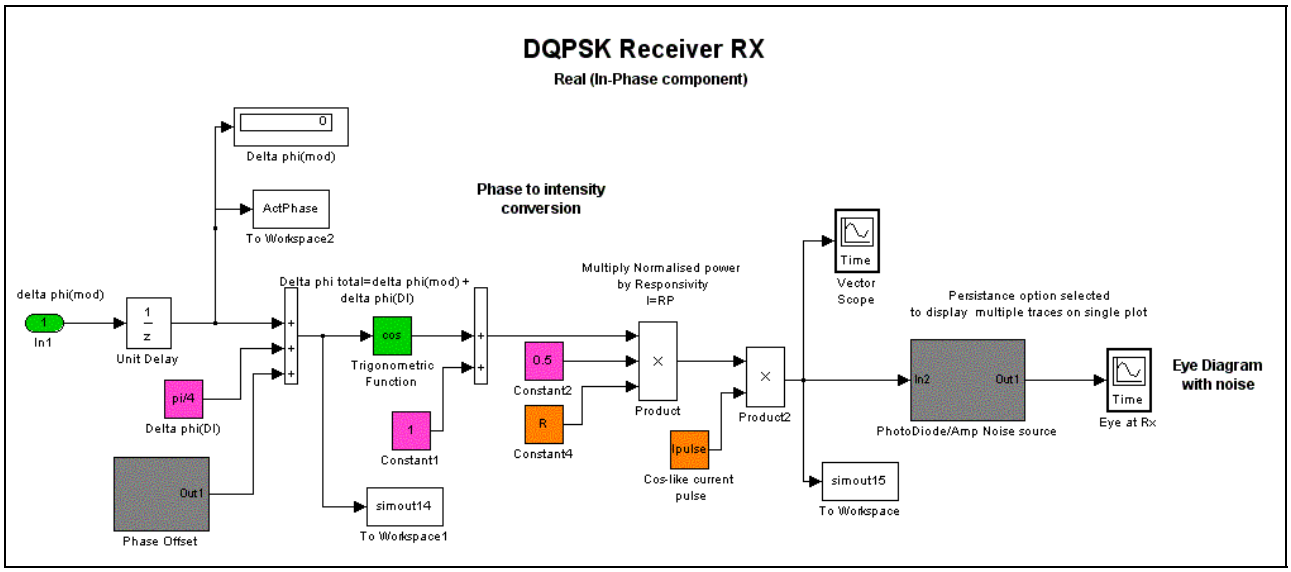

Figure 20: Receiver model including noise sources

Mach-Zehnder Delay Interferometer model component

In *Figure 8* it can be seen that at the input of Receiver block, there is a *'Complex Phase Difference'* block. The purpose of this block is to deduce the overall phase difference between the received symbol that has been phase encoded and the reference signal given by the state of the optical carrier prior to modulation directed from the transmitter. The output of this block is constantly varying due

to the periodic nature of the optical carrier; however we eliminate this problem by sampling this 'Phase difference' value every 100 ps for 10Gb/s operation. This sampling is done by the first unit delay block observed above in ***Figure 20***. The reasoning behind this operation is to extract the optical phase difference (differential phase information) between adjacent symbols and to thus perform the phase to intensity conversion operation of the MZDI. This characteristic of the MZDI allows for the phase coded information to be converted into detectable intensity information[15]. Since we are only considering the real component of the received signal we need to add and extra $+\pi/4$ phase shift to the phase difference, $\Delta\phi_{\text{mod}}$ of the signal received. As shown in figure 7, when considering the four possible phase states of the DQPSK signaling format *{0, π/2, π, 3π/2}* and adding DI phase of $\pi/4$, the overall phase difference takes 'equivalent' values of either *{π/4 or 3π/4}*. Given the MZDI transfer characteristic this leads two possible 'Intensity mappings' as shown in *Figure 21*. From the values of phase obtained here we determine the corresponding output intensity of the MZDI by its characteristic expressed as:

$$I = 0.5\cos\left(\Delta\phi_{\text{mod}} + \Delta\phi_{DI} + \delta\phi_{DI}\right) + 0.5$$
$$\text{where } \Delta\phi_{DI} = +\frac{\pi}{4} \qquad (12)$$

The final term, $\delta\phi_{DI}$ in (12) is referred to as the *phase offset*. This additional phase originates from the MZDI and adds extra phase noise to the system. This effect is shown to reduce eye opening and hence degrades system performance. We have interpreted this effect as being a result of the instability of the heaters which induce the required $+\pi/4$ phase shift, thus producing random values about this bias value. We have modeled this effect in Simulink by assuming a maximum possible value of $\delta\phi_{DI}$ and use a random *'Gaussian White noise generator'* with small variance to represent this phase offset noise. The effects of this phase offset as described earlier are shown in *Figure 21*.

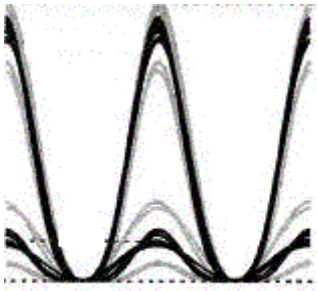

DQPSK

***Figure 21**: The darker eye traces in this eye diagram are the expected traces, the light traces are after phase offset noise due to the instability of the "phase tuning" heater.*

Figure 22 shows the Simulink model developed to simulate phase offset noise of the MZDI.

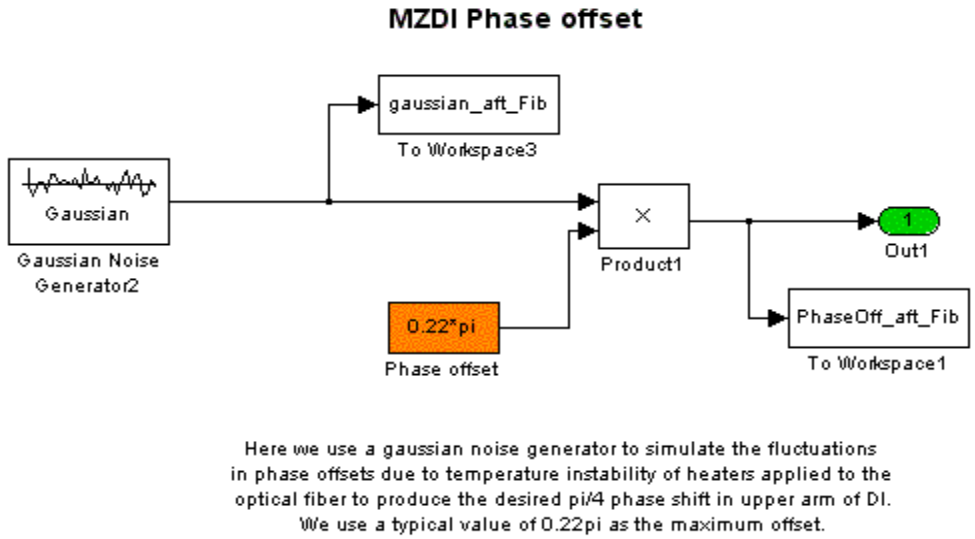

***Figure 22**: MZDI phase offset noise model*

Referring back to *Figure 21* we take the cosine of this total phase value, add 1 and multiply by ½ to give the intensity corresponding to the MZDI characteristic.

The Photodiode Model component

Now that we have the intensity equivalent of the phase difference, we need to represent the optical to electrical conversion performed by the single-ended photodiode. From (2) we need to multiply the power, effectively the value just obtained from the MZDI, by the photodiode Responsivity, $\Re$. We use a value of 0.5A/W obtained from *Discovery Semiconductor Inc DSC10H PIN* photodiode datasheet. Evaluating the average photocurrent given a signal of power *P* from the MZDI using (2), we obtain one value between 0 and 1 as normalized current is assumed. Since we would like to asses the eye diagram generated by the received 'real' bits, we approximate the eye diagram pattern by the I_{pulse} variable in our simulations. Since the MZDI characteristic is cos-like, we assume the current waveforms forming the eye-diagram are cos-like also. The I_{pulse} variable is expressed as:

$$Ipulse = -0.5\cos(t)+0.5 \quad ; \ 0 \le t \le 2\pi; \tag{13}$$

We thus multiply the value of current obtained by (12) as shown in ***Figure 23***. As each symbol is received and demodulated a waveform of type I_{pulse} with peak value given by (2) will appear in the *Time Vector Scope.*

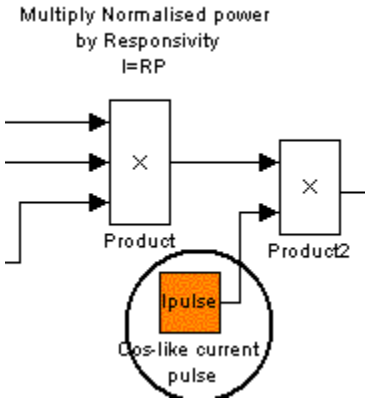

Figure 23: I_{pulse} variable simulates current waveform

Finally, to complete the practical nature of the simulations we add the photodiode and amplifier noise. These noise sources are superimposed on the current waveforms.

Photodiode/ Amplifier Noise component

The detection of transmitted lightwaves is performed primarily by the photodetector. In most instances, the received optical signal is quite weak and thus electronic amplification circuitry is used, following the photodiode, to ensure that an optimized power signal-to-noise ratio (SNR) is achieved[26]. This power signal to noise ratio is calculated as follows:

$$\frac{S}{N} = \frac{I_{sig}^{\ 2}}{\left\langle I_{noise}^{\ 2} \right\rangle} \tag{14}$$

Here we denote I_{sig} as the photocurrent and $\left\langle I_{noise}^{\ 2} \right\rangle$ as the mean squared noise contributions from the photodetector, the reason why we consider the mean squared noise will be explained later. Since one of the primary objectives is to best model optical components used in real experimental conditions the effects of noise is modeled. In particular the PIN photodiode and receiver total noise are calculated and superimposed over the ideal photodiode signal current. Three sources of noises include: the quantum shot noise i_{sh}, the PD dark current noise i_{dk} and the thermal (Johnson) noise i_{th}. The total current generated by the photodiode when optical power falls on it is expressed by:

$$
\begin{aligned}
&i_{total} = i_{sig} + \sqrt{\left\langle i_{noise}{}^2 \right\rangle} \\
&where \\
&\left\langle i_{noise}{}^2 \right\rangle = \left\langle i_{sh}{}^2 \right\rangle + \left\langle i_{th}{}^2 \right\rangle + \left\langle i_{dk}{}^2 \right\rangle
\end{aligned}
\tag{15}
$$

It has been demonstrated that both the shot noise and dark current noise contributions from the bulk material of the photodiode follow a Poisson process, and is thus random. As a result we consider the mean squared of these noise sources for our calculations. The noise sources are expressed mathematically by:

$$
\begin{aligned}
\left\langle i_{sh}{}^2 \right\rangle &= 2qI_{sig}B \\
\left\langle i_{dk}{}^2 \right\rangle &= 2qI_{dk}B \\
\left\langle i_{th}{}^2 \right\rangle &= \frac{4k_BTB}{R}
\end{aligned}
\tag{16}
$$

where I_{dk} is assumed to be the average dark current obtained from the *Semiconductor.Inc DSC10H PIN* photodiode datasheet (25nA), B is the photodiode 3dB bandwidth, k_B is Boltzmann's constant, T is the absolute temperature (^oK) and R is the photodiode load resistor, assumed to be 50Ω or ultra-wide band receiver. A total normalized mean squared noise of $\left\langle i_{noise}{}^2 \right\rangle = 4.44 \times 10^{-4}$ is determined.

The need for amplification of the photodiode current is critical to ensure correct retrieval of data, we have thus implemented a gain related to an amplifier selected from MITEQ manufacturer product list[2] with a noise figure[3] (NF) of 0.5dB which translates to an 11% (of max current = 19.11 normalized) amplifier noise addition to the current waveform. This amplifier also has a 33dB gain which translates to a power gain of 44.67. The addition of the photodiode noise to the photocurrent, the amplifier gain and addition of amplifier noise models developed in Simulink are shown in *Figure 24*. The values of noise calculated above are maxima and are assumed to have a Gaussian distribution.

[2] Miteq; Model# AMF-2F-00250050-05-10P
http://www.miteq.com/micro/amps/amfamps/c23b/ampmodels/lownoiseframeset.html see Appendix 8.2

[3] $NF = 10\log_{10}\left(\frac{SNR_{beforeAmp;no-noise}}{SNR_{afterAmp;with-noise}}\right)$

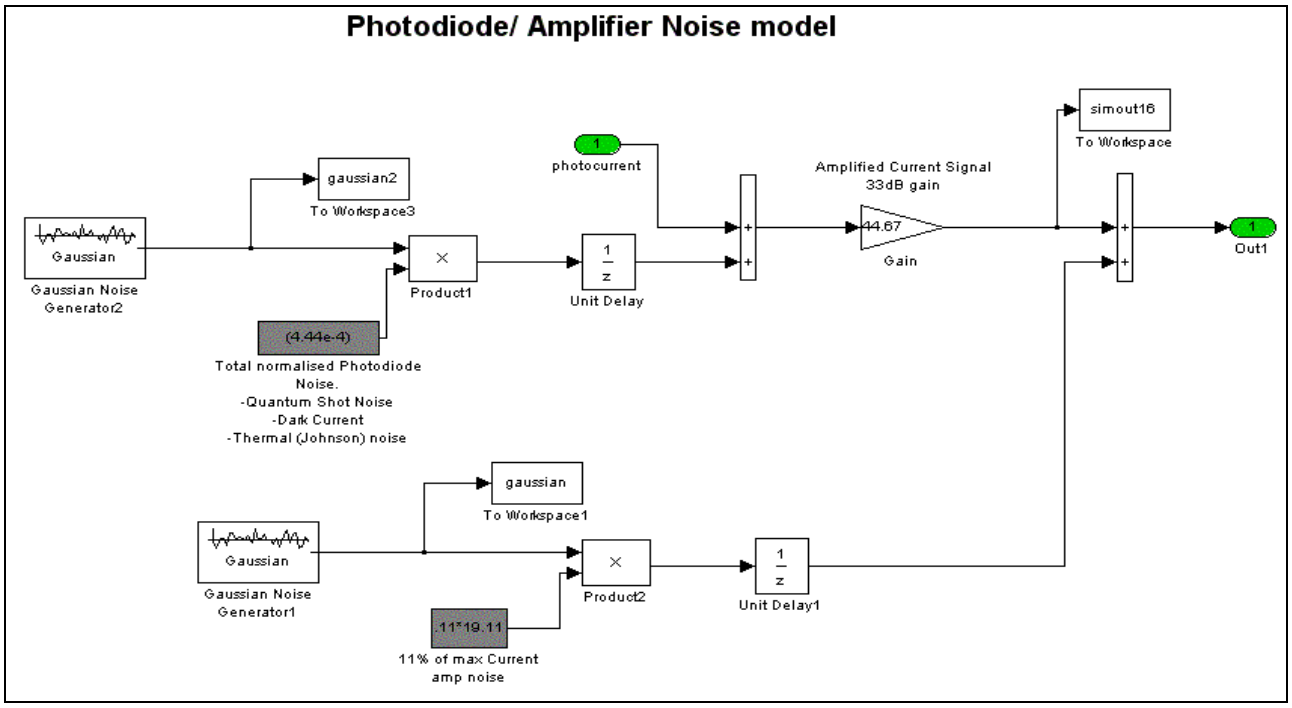

***Figure 24**: Simulink photodiode and amplifier noise contributions added to photocurrent.*

5 Single Channel DQPSK system simulator

In this section of the document we state the necessary steps required to operate the single channel DQPSK optical fiber communication simulator. Our intentions are to provide all the necessary instructions on how to alter the simulator for optimum individual requirements. The flexible nature of Simulink, and thus this simulator allows the system to be customized to handle different fiber types, and can with simple alteration of the transmitter and receiver even implement the DPSK modulation format. This simulator was designed for DQPSK transmission in mind and is thus unable to support other modulation formats. However certain components from this simulator may be used to generate new simulators implementing alternative modulation formats.

This section present some results performed for assessing the overall system performance. It includes an analysis of the effects of chromatic dispersion induced by the fiber model. We investigate the effects of dispersion compensation fibers in the transmission link, in particular the effect of phase distortion by comparing the received phase difference to the expected phase difference originally encoded in the symbol. We also perform BER testing derived from the eye diagram generated by the Q-factor.

5.1 Operating the DQPSK OFC Simulator

The simulator operation has been designed based on a previous Simulink simulator design[22]. This report uses the principles of operational simplicity to allow for ease of operation and flexibility for the user. It is important that prior to running any simulations the initialization file contained within the simulation package be run. To begin running any simulations open Matlab™ 6.5 and open the file *initialise_optical_simulator_DQPSK.m* which is included in the Appendix. Some of the variables made available to the user for alteration include transmission bit-rate, dispersion factors and length of various fibers. By localizing all the variables used in the simulator in the m-file allows the user to make system or fiber alterations to the m-file and consequently result in an update of variable in the simulator once the simulator is re-initialized. All the variables declared in the initialization file will automatically be placed on the Matlab workspace. If these variables are not declared and defined prior to simulation run-time Simulink will generate errors. After running the initialization file, the DQPSK simulator model is automatically open, provided the user has specified the correct file location of the simulator file named *SingChanDQPSK_sim.mdl,* in the open command at the end of the m-file.

Now that the simulator has been initialized with all the fiber parameters and bit-rates etc, simulations can now begin.

IMPORTANT:

ENSURE THAT THE SCREENSAVER OPTION (IN CONTROL PANEL) IS TURNED OFF DURING SIMULATION RUN-TIME. KEEP THE EYE DIAGRAM WINDOWS ON TOP (AND UNCOVERED BY ANY OTHER WINDOWS) DURING SIMULATION RUN-TIME AND ALLOW SIMULATIONS TO CONCLUDE TO VIEW FULL EYE DIAGRAM.

To begin simulations click the  button on the Simulink toolbar, or click Simulation → Start. All the vector scopes, spectrum scopes and eye diagram windows are open. These windows present a graphical representation of the processing of data in real-time. Users can observe certain phenomena whilst also acting as a good guiding tool to troubleshoot any underlying system problems. During the simulations, data generated by the simulator is stored in the Matlab workspace variables. At the conclusion of the simulations this data can be analyzed and processed in Matlab to present other graphical representations of the results as desired.

To observe or alter the contents of each sub-block in the simulator model simply double click on the block of interest and the contents are revealed.

5.2 DQPSK optical simulator performance

The SOAST has been designed to be as flexible as possible to allow users modifications of system parameters, and to add or remove simulation blocks as desired. For example one may need to alter the current state of the simple transmission peer to peer transmission link by forming long-haul transmission with optical amplifiers and improved dispersion management. The applications of this simulator are left to be user specified. However for testing purposes and to give an indication of the proper operation of the 10 Gb/s single channel DQPSK system, we consider two system configurations.

One utilizes standard Tx and Rx whilst *assuming SMF type* with *no dispersion management*, the *other includes dispersion management* in the form of a *dispersion compensating fiber (DCF) module.* Thus the overall transmission span is 96 km. This fiber span corresponds well with the typical transmission distance considered in practice (<100 km). The system parameters used in the following simulation correspond to the values specified in the *initialise_optical_simulator_DQPSK.m* file shown in the Appendix 8.1. After running this initialization file and loading all variables into the Matlab workspace the simulations can now begin (after clicking the run,  button), the following window scopes (refer *Figure 26*) open to display appropriate data signals. The simulator displays the following window scopes in real time:

- MZIM and PM NRZ electrical random data driving signal;
- Optical power spectrum of single channel (193.4 THz ≡ 0.1934 PHz; PHz = 10^{15} Hz) post transmitter and at receiver inputs;
- Single photodiode electrical current eye diagram scope at the receiver with no photodiode/amp noise; and
- Single photodiode electrical current eye diagram scope post transmitter, and at the receiver superimposed by all noise sources.

Other time scopes in the simulator system can be manually opened during simulation run-time. A large number of windows have been assigned to open automatically. The importance of certain data representation is left to users and can be disabled if required. However the scopes selected to be displayed (*Figure 25*) present a good overview of the current system design and allow, in particular, BER estimation directly from the eye diagram traces.

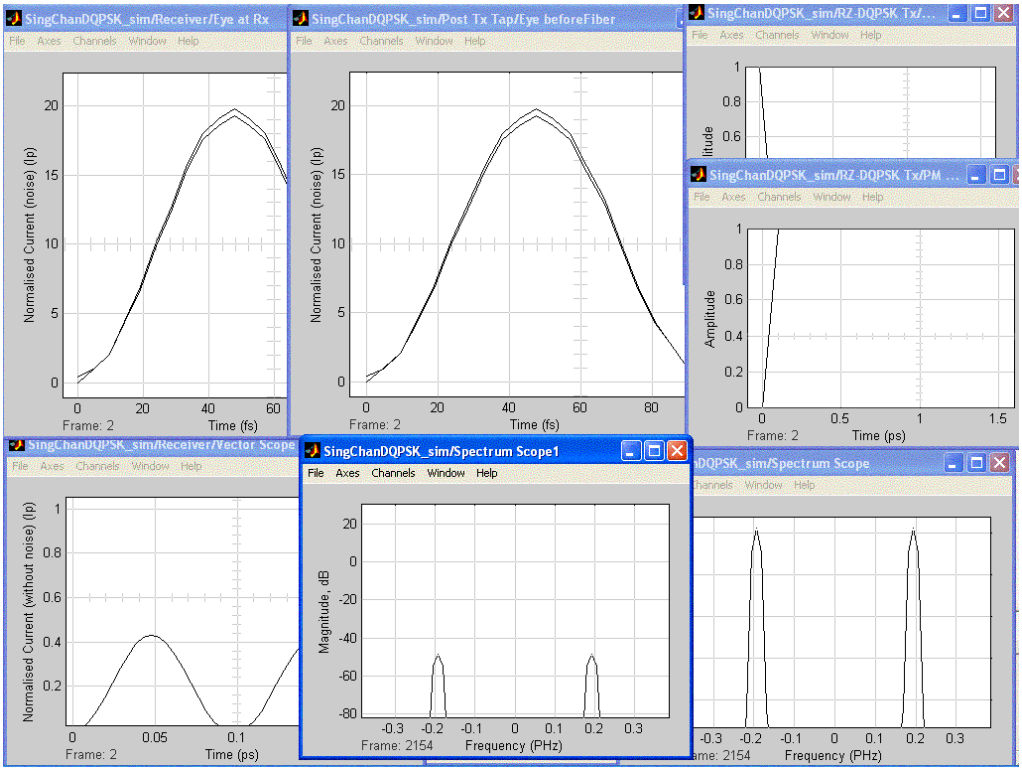

***Figure 25**: Full view of all window scopes displayed during simulations*

Figure 26 shows the RZ pulse carving incorporating the optical carrier in the time domain on the left, note that the magnitude of the carrier is a maximum. The scope figure on the right is the spectrum of the optical carrier, this spectrum displays the spectra expected by theory from a sinusoidal signal of frequency 193.4 THz, ideally two peaks centered on 193.4THz or equivalently 0.1934 PHz.

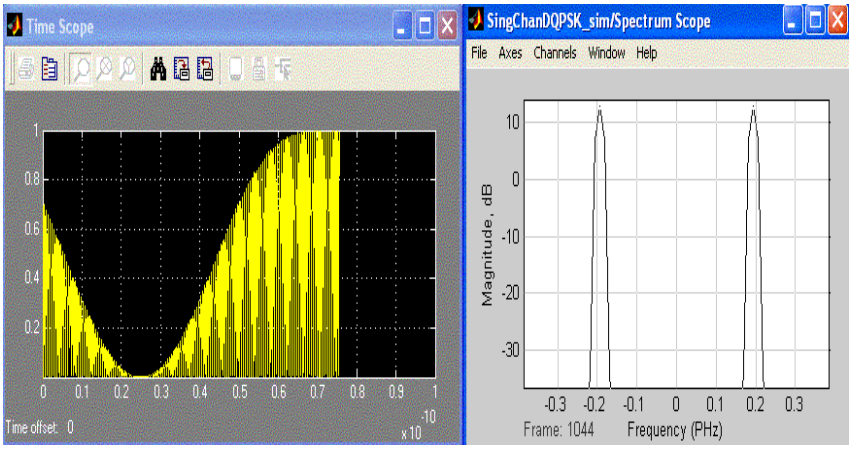

(a) (b)

***Figure 26**: Spectrum scope outputs of (a) RZ pulse carving with 193.4THz optical carrier (b) Optical spectrum.*

Since the spectrum of the optical carrier displays both its magnitude and frequency components, we expect the magnitude of the spectral peaks to reduce and increase in synchronization with the RZ time domain pulse magnitude variation. This effect is observed during simulation run-time.

Figure 27 is a representation of the NRZ electrical bit pattern generated by the simulator with 32 bits (2x16 bits) in total to be encoded via DQPSK modulation format. The first plot (a) displays the data driving the MZIM and the second (b) the PM in the Tx setup. Note that Simulink displays discrete data with lines interpolated between them. Thus a series of 0's and 1's will appear joined in some ways. As noted earlier, the nature of the DQPSK modulation format allows 32 bits to be transmitted however we only effectively transmit 16 symbols (i.e. 2 bits per symbol).

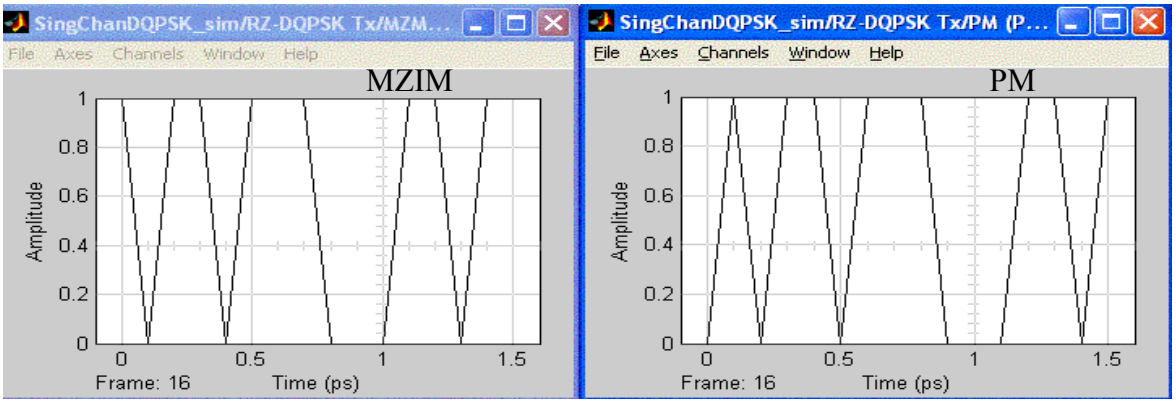

(a) (b)

Figure 27: Example of NRZ Electrical bit pattern generated by the simulator driving the MZIM and PM

Table 2 presents the notion of di-bit coding. With reference to *Figure 27*, the first 3 di-bits coded are tabulated.

MZIM driving bit	PM driving bit	Di-bit code	$\Delta\phi_{\text{mod}}$
1	0	10	π
0	1	01	π/2
1	0	10	π

Table 2: Examples of di-bit coding in relation to Figure 27.

In the '*Post Tx Tap'* block an *IdealPhase* workspace block is added and likewise an *ActPhase* workspace block in the *'Receiver'* block. These blocks have been intentionally inserted into the simulator to allow for comparison between the expected phase difference, $\Delta\phi_{\text{mod}}$ (stored in the *IdealPhase* block), based on the 256 di-bit sequence to be encoded (refer *Figure 7*) and the phase difference determined by the receiver (stored in the *ActPhase* block*)*. What we propose here is a simulation test that gathers phase difference data at the receiver and compares it to the true phase difference initially encoded at the transmitter, and estimates the BER of the system from the eye diagram formed. This will allow the effects of data/ phase corruption due to fiber dispersion implemented in our fiber model to be realized. These tests also emphasize the need for dispersion management with respect to maintaining transmitted symbol integrity.

First consider a single channel DQPSK OFC transmission link using 80 km of SSMF without DCF modules/models in place. We compare the expected phase difference $\Delta\phi_{\text{mod}-\text{expected}}$ with that detected at the receiver $\Delta\phi_{\text{mod}-\text{receiver}}$. Later we examine the eye diagram and calculate the associated BER. The phase comparisons for a random (2 x 2^4) 512 (or 256 di-bit) bit sequence is shown in ***Figure 28***. Note that for display convenience the first 16 di-bit phase differences of 256 are shown to reduce cluster of the display. The main purpose here is to emphasize the need of a DCF module.

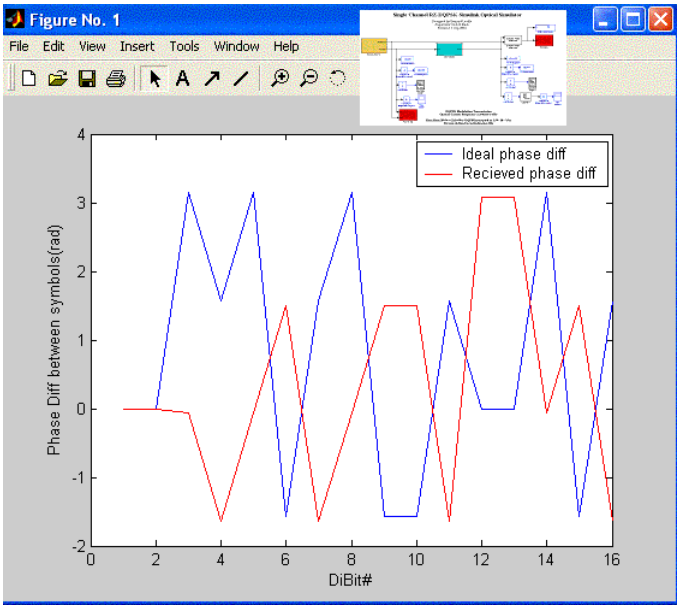

Figure 28: Phase comparison between the expected (transmitted) and received phase differences for 16/256 di-bit transmission over SMF fiber link (No Dispersion Compensation).

As can be seen in *Figure 28* when there is no dispersion compensation management placed in the fiber link, dispersion effects of the fiber corrupt the differential phase of the transmitted symbol. The phase difference between adjacent symbols detected by the receiver (Red plot) is on all occasions incorrect. This results in incorrect phase to intensity conversion by the MZDI at the receiver and thus would effectively lead to incorrect data recovery had we designed a data recovery component in our simulations. The high degree of bit recovery error is an indication of the need for dispersion management. Later, we investigate the positive effects of dispersion management by inserting a DCF module into the fiber link and perform the same test as above.

We now examine the BER calculations derived from the eye diagram formed at the output of the receiver model given a 2^4 (256) random bit encoded sequence. We consider the eye diagram generated by 256 traces generated by the photodiode model to be sufficient to adequately measure the BER. However, for more comprehensive tests, a 2^{31} -1 random bit sequence (PRBS) would be required. It should be noted that this PRBS consequently consumes a much longer processing time, Thus for 2^{31} -1 PRBS bit pattern, we suggest removing as many data storage blocks (i.e. *to workspace* blocks) and unnecessary display blocks from the simulator as possible to reduce the possibility of insufficient memory difficulties and reduce calculations for the displays not essential to the user. The eye diagram, shown in *Figure 29* is without any electronic or photonic noises and

MZDI phase offset additions and Figure 33 is complete with inserted photodiode, amplifier noises and MZDI phase offset. We use *Figure 29* for BER calculations. Note that only one bit period of the eye pattern trace is observed. The extended eye diagram can be viewed by double clicking on the '*Eye at Rx'* vector scope and changing the 'number of frames' field to the number of eyes as desired.

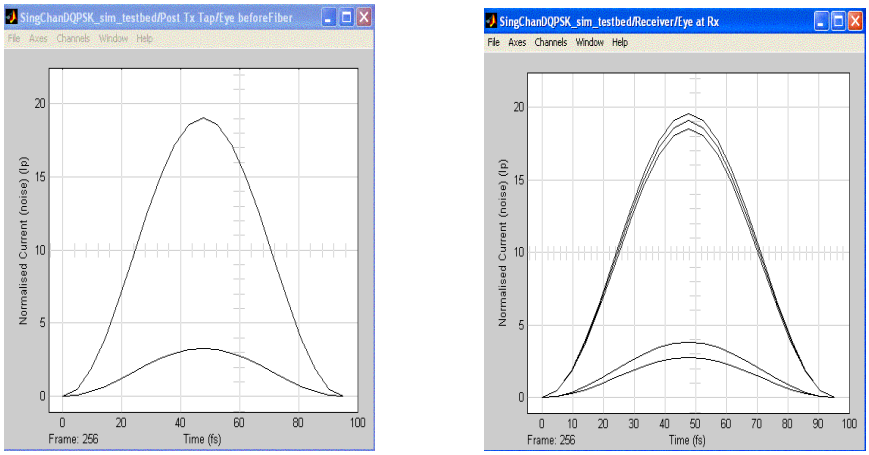

(a) (b)

Figure 29: Electrical current eye diagram generated before fiber (a) and at Rx(b). Using SMF link, without DCF, no PD and amplifier noises and no MZDI phase offset. This eye effectively shows the dispersion effects of SMF alone on the eye closure and thence on BER. The phase to intensity converted by the receiver no longer has two distinct levels as on the left (a).

We have added *Figure 30* below for comparative purposes to show the effects of noise and MZDI phase offset on the eye closure and thus BER performance measures.

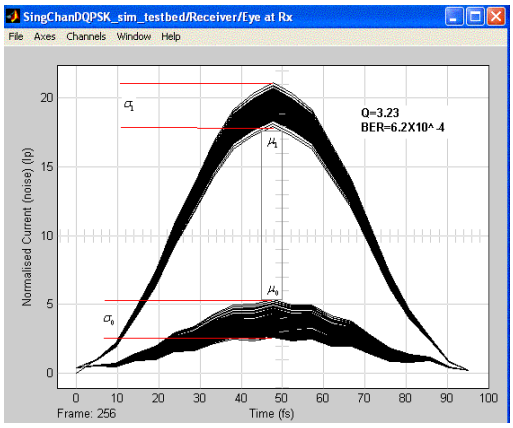

***Figure 30**: Electrical current eye diagram generated at Rx with SMF link, No DCF inserted with PD and amp noise added.*

Note that we have used the approximation to the BER. Furthermore for OOK systems we use this approximation to indicate our simulator system performance. The Q-factor from the eye diagram can be evaluated as follows [25]:

$$Q = \frac{\mu_1 - \mu_0}{\sigma_1' + \sigma_0'} \tag{17}$$

where $\mu_1 - \mu_0$ is the magnitude of the eye opening shown by the inner square in *Figure 30*. σ_1' *and* σ_0' are fractions of σ_1 *and* σ_0 whose values are shown. They are defined, for Gaussian pulse shapes as:

$$\begin{aligned} \sigma_0' &= 0.68\sigma_0 \\ \sigma_1' &= 0.68\sigma_1 \end{aligned} \tag{18}$$

Assuming a Gaussian noise distribution, the BER is derived from (16) or Q as [27]:

$$BER = \frac{1}{2} erfc\left(\frac{Q}{\sqrt{2}}\right) \tag{19}$$

For the case of no dispersion management we have calculated a BER of 6.2 x 10^{-4} [28]. We thus now include the DCF fiber module in series with the SMF fiber and look at the positive effects of exact phase difference detection and improved BER. For the non-dispersion compensating we can observed the phase difference detected at the receiver in comparison to the initial phase difference encoded by the transmitter for the first 16 di-bit sequences.

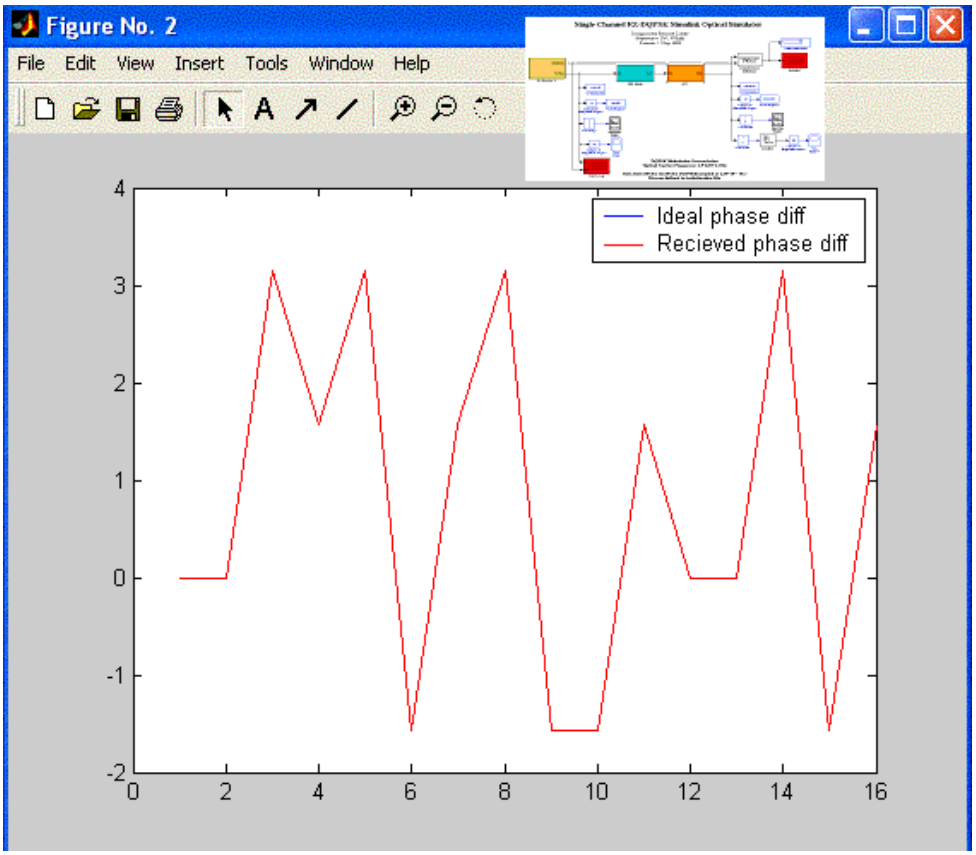

***Figure 31**: Phase comparison between the expected (transmitted) and received phase differences for SMF fiber link with DCF compensation.*

As seen in *Figure 31* with dispersion compensating with dispersion factor of -85 ps/nm.km and 16 km long DCF, the dispersion of the transmitted signal induced by the SMF is completely equalized. The phase difference at the receiver $\Delta\phi_{\text{mod}-\text{receiver}} = \Delta\phi_{\text{mod}-\text{expected}}$ on all occasions implying *correct data retrieval*. Since the dispersion factor of the DCF is approximated to exactly equalize all dispersion effects of the SSMF we expected an error-free eye diagram at the receiver. We obtain the following eye diagram traces as shown in ***Figure 32***and derive the Q-factor and its corresponding BER.

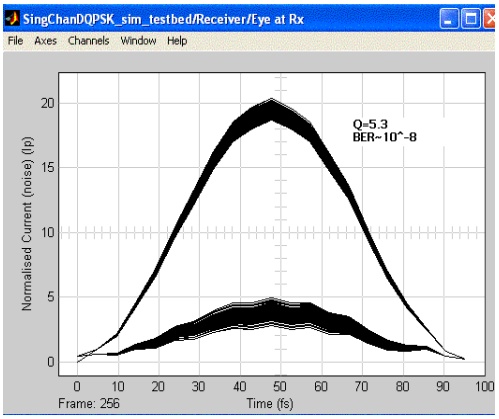

Figure 32: Electrical current eye diagram generated at Rx with SMF & DCF inserted with PD and amp noise added

The BER of 10^{-12} achieved for 10 Gb/s single channel DQPSK dispersion compensated transmission system is considered error-free for single photodiode detection schemes. As mentioned earlier our intentions are to compare our simulated results with those published and experimentally conducted. In some published works BER values extend to as low as 10^{-5} regions[18] for single PD detection. In practice, it is more common to use balanced detection receiver configurations they have shown to offer a 3 dB power improvement.

If balanced detection is implemented, the BER would be expected to be 10^{-15}. However we must note that the added noise implemented into our simulations are derived from maximum values and the phase offset incurred in the MZDI has been intentionally selected large to emphasize the effects of phase offsets. For future work we suggest modifying the noise values to controlled minimum operational conditions and re-calculate the BER.

Our final test investigates the effects of varying the dispersion factor of the DCF on the BER. The corresponding eye diagram traces obtained for $D(\lambda) = -75$ *ps/nm.km* and $D(\lambda) = -65$ *ps/nm.km* are shown below along with the calculated Q factor and BER values using conventional estimation methods.

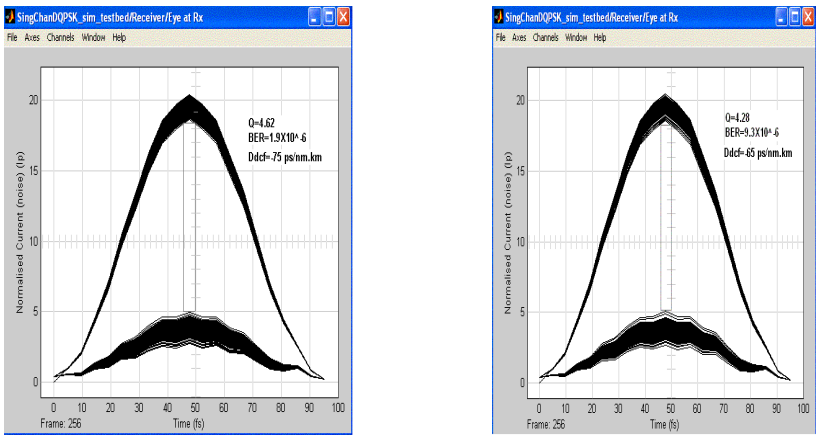

***Figure 33**: Electrical current eye diagram generated at Rx with (a) $D(\lambda)_{DCF}$ = -75 ps/nm.km (b) $D(\lambda)_{DCF}$ = -65 ps/nm.km*

From *Figure 33* we can see that increasing the dispersion factor of the DCF from -85 to -75 ps/nm.km reduces the BER from the order of 10^{-12} to 10^{-11} and slightly more when $D_{DCF}(\lambda)$ = -65 ps/nm.km, thus allowing the system to become more prone to errors at detection. These simulations have presented an important fact and show the importance of simulating transmission systems prior to physical implementation. In these tests, the simulator has provided us with important information in regards to the effects of dispersion on the BER. In the case of correct dispersion management the BER of the order of 10^{-8} brings the BER value obtained in these simulations to a value that is comparable with the results obtained in installed systems [18] for single ended detection.

We note also that our simulations have not included the practical limitations of receiver sensitivity. We have assumed in our simulations that the attenuation of the transmitted signal in the fiber exists. However the power limit that the receiver model can detect has not been enforced.

We have stated that the DQPSK simulator has been designed to simulate an advanced single channel DQPSK optical fiber communication system. We now briefly compare the eye diagram results achieved from the simulator to those obtained experimentally as reported. We make the comparison visually via the eye diagrams shown in *Figure 34*. Note that for the simulated eye (a) we have set the eye diagram pattern to display one bit interval only.

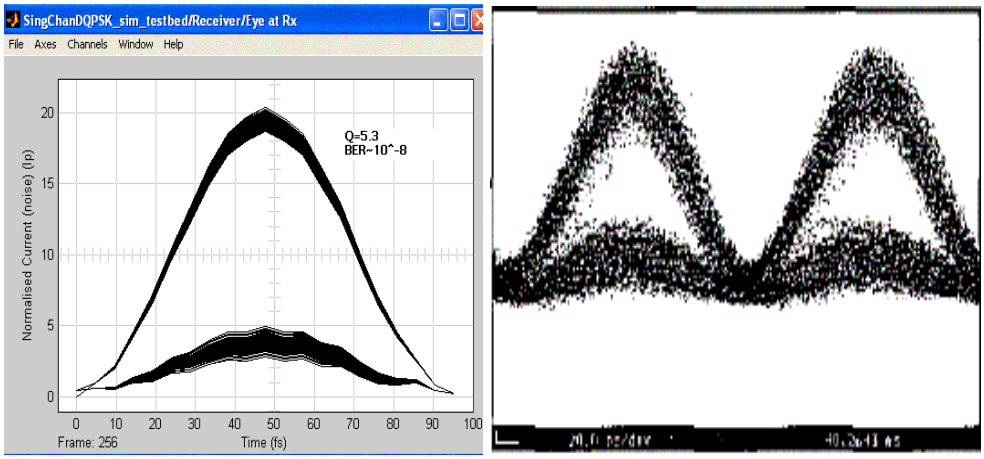

(a) (b)

***Figure 34**: Single-ended simulated eye diagram (a), Eye diagram source obtained via experimental investigation from literature search using a similar transmitter configuration to the simulator (b)[18].*

From *Figure 34* we can see the eye pattern generated closely resembles the eye pattern obtained in experiments. These results emphasize our motivation to closely model a simulator which is capable of generating results and producing the practical features present in a real OFCS. For completeness we present the eye diagram generated for 10 Gb/s RZ-OOK transmission over 48 km (as apposed to 96 km for equivalency) generated by the MOCSS 2000[1] shown in *Figure 35*.

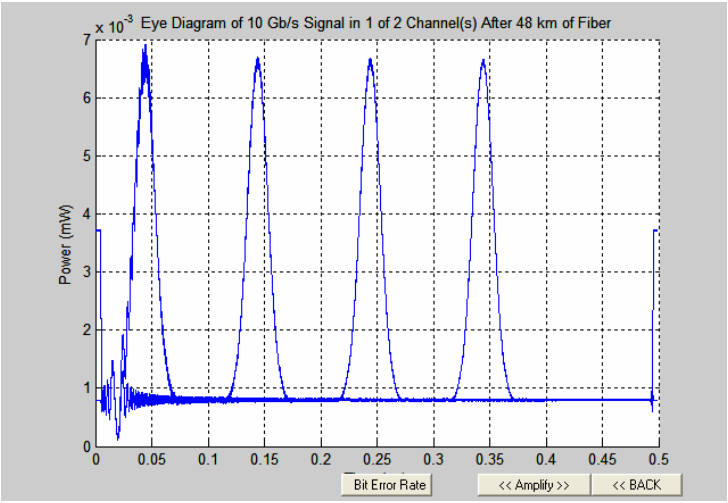

***Figure 35** MOCSS 2000 (Matlab Simulator): 10 Gb/s RZ-OOK transmission over 48 km.*

6 Concluding remarks

In this report we have considered the three main components which form a simple, yet typical single channel optical fiber communication link including the transmitter, optical fibers –standard and compensating types and receiver. To our knowledge this optical DQPSK simulator is the first to have been reported and developed in the Matlab™ Simulink platform. The flexible nature of Simulink and its wide range of pre-designed blocksets allow several important features for implementation of optically amplified transmission systems.

Although the development of the Simulator in the Simulink platform can be time consuming, gaining an understanding of the physical carrier phases of the DQPSK system is considered as the most challenging tasks. It has been found that the DQPSK modulation format can and has been implemented in different ways using alternative hardware ranging from integrated lasers and dual drive Mach-Zehnder modulator devices to simple configurations using MZIM's and PM's.

We have stated that the DQPSK modulation format offers twice the bandwidth compared to conventional OOK. Apart from the di- bit coding aspect of this modulation format and the increase in spectral efficiency (b/s/Hz) that would be observed in DWDM systems, presentation of results that prove the superiority (to OOK) of this format. In this simulator we have modeled for the detection case using a single PD. Balanced detection or receiver diversity would significantly improve the BER performance by at least 3.5 dB. We have also included the eye diagram results for 10 Gb/s RZ-OOK from the MOCSS 2000 optical simulator, updated recently for comparison and for completeness.

Regarding the fiber propagation model, we have not implemented in this part but reserved for Part V, the fiber split step Fourier model. However the linear fiber model as a low pass filter is proved to present sufficiently accurate on dispersion effects provided the total optical power is below the nonlinear SPM threshold. The simplicity to develop in the Simulink environment is also a positive factor. Due to the good linkage developed between all parts of the series the 10Gb/s DWDM optical fiber systems, the optimization of various block components are achieved.

The development of the simulator for 10 Gb/s and 40 Gb/s single channel DQPSK has been proposed to provide, unlike other commercial packages such as VPI Systems, the most effective and simplified simulation. This simulator has, as required, simulated the most complex modulation format of the family of optical modulation techniques proposed in literature of digital optical

communications. The nature in which the simulator has been designed in Simulink allows for future development of the DPSK (Differential phase shift keying) and other optical modulation formats, e.g. multi-level M-ary schemes. This technique has also been well explored in practice and derives from the same differential phase coding principle as DQPSK. To implement this system, the phase modulation (PM) of the transmitter would be omitted and one pair of MZDI at the receiver would be required for the in-phase and quadrature phase channels. In addition, the $\pi/4$ phase shift incorporated into the MZDI upper arm would be set to zero. Because of the 0 and π symbol phase states allowed, the eye diagram is expected to form a constellation and hence improvement of the receiver sensitivity, resulting in higher Q-factors and thus lower BER. Although higher sensitivity would be achieved, this technique comes at the expense of only transmitting 1 bit/symbol as opposed to 2 bits/symbol of the DQPSK system.

As commented earlier, the DCF modules have been implemented in SOATS for management of fiber dispersion effects to improve the overall system BER. This dispersion management technique is commonly used in practical systems. The simulator model reported here has considered only the transmission fiber, spanning a total length of 96 km. Multi-span long-haul dispersion managed transmission can be extended without difficulty incorporating EDFA pre-amplifier and booster amplifiers. Several spans of SMF and DCF fiber and optically amplified models can be cascaded. The combinations of SMF and DCF would, in practice need to be compensated by optical amplifiers (~every 80 to 100 km). EDFAs or Raman OAs have been currently developed and would be integrated in SOATS. Non-linear effects of fiber propagation and receiver sensitivity would positively enhance the capability of SOATS. This simulation system can be extended and used as a useful tool for assessing designs of Super DWDM optical fiber networks implementing in particular, DQPSK systems, thus allowing transmission capacities to be simulated to the high Tb/s capacity.

From the optical components used to construct the transmitter, the importance of system design simplicity to implement complex modulation formats such as the DQPSK format has been realized. The total transmission capacity of advanced optical fiber communication system is extending into the Tb/s. Furthermore considering the recent increasing demands of data bandwidth, system designs such as DWDM, which increase channel capacity using existing available photonic hardware is of significant importance. Apart from the system configuration, modulation formats used to transmit data can also increase data transmission capacity with its effective bandwidth, truly single side

band. It is thus now possible to remove the limitations of hardware and extend to the signaling aspects to improve transmission capacity.

We have demonstrated a 20 Gb/s (2 X 10Gb/s) single channel optical DQPSK simulator which is capable of doubling the bitrate compared to conventional OOK signaling techniques. The simulator has been developed in the Matlab subsidiary program simulink and due to its nature can easily be altered to suite the user specifications or to improve system optimization. All-optical components necessary to transmit, propagate and decode/ receive the transmitted bit stream have been implemented in the simulator along including the superposition of added noises etc. Transmitter components include the MZIM and PM along with the optical carrier and electrical bit stream PRBS generators. The fiber has been developed using a linear LPF model which only takes into account the linear dispersion effects of optical fibers. We have shown that without appropriate dispersion management, the phase information coded in adjacent symbols is corrupted. We have also demonstrated that the simulator is a good tool for altering system specifications such as dispersion factors of fiber and providing quick results for performance comparisons.

The simulator is extended in the future to simulate dense and super-dense WDM long-haul transmission systems. This work has provided the framework for individual channels that would compose the DWDM system. Given that we have successfully demonstrated 20 Gb/s transmission using a single DQPSK channel with a BER of 10^{-12} an extension to the Tb/s would become a possibility.

7 REFERENCES

[1] L. N. Binh, Lam,D., Chi, K.Y., "Monash Optical Communications Systems Simulator," ECSE Monash University, Melbourne Australia 1997.

[2] L. N. Binh, and Li, C.H.,, "EDFA Simulink Simulator," Monash university, Melbourne Australia 2004.

[3] B. Zhu, ""3.08 Tbit/s (77 ´ 42.7 Gbit/s) WDM transmission over 1200 km fibre with 100 km repeater spacing using dual C- and L-band hybrid Raman/erbium-doped inline amplifiers"," *Elect. Lett*, vol. 37, 2001, 21 June.

[4] E. Yamada, " "106 channel 10 Gbit/s, 640 km DWDM transmission with 25 GHz spacing with supercontinuum multi-carrier source"," *Elect. Lett.,*, vol. 37, 2001.

[5] C. Wree, " "RZ-DQPSK format with high spectral efficiency and high robustness towards fiber nonlinearities"," University of Kiel, 2002.

[6] A. Carena, "'A time domain optical transmission system simulation package accounting for Nonlinear and Polarization-related effects in fiber'; ." *IEEE J. Selected Areas in Communications*, vol. 15, 1997.
[7] M. J. N. Sibley, *Optical components and systems*, 2nd ed: J.Wiley, 1995.
[8] L. N. Binh, *ECE 4405 Lecture Notes on Optical Communications Systems*. Melbourne, Australia: MiTec, 2003.
[9] J. T. Gallo, " 'Optical Modulators for fiber systems';," presented at IEEE GaAs Digest;p. 145, 2003.
[10] A. F. Elrefaie, "Chromatic Dispersion limitations in coherent lightwave transmission systems';," *IEEE J. Lightwave Technology*, vol. 6, 1988, May.
[11] Corning, *Corning :Fiber-Optic Technology Tutorial; The International Engineering Consortium*.
[12] L. N. Binh, ""An introduction to optical planar waveguides and optical fibers";," Department of Electrical and Computer systems engineering; Monash University, 1997, pp. 20-21.
[13] S. V. Kartalopoulos, *"Introduction to DWDM technology: Data in a rainbow"*: J Wiley, 2001.
[14] K.-P. Ho, "Raised Cosine function in time domain as defined "Spectrum of externally modulated optical signals," *IEEE J. Lighjtw. Tech.*, 2004.
[15] H. Kim, " H. Kim "Robustness to Laser Frequency Offset in Direct-Detection DPSK and DQPSK systems"," *IEEE J. Lightwave Technology,*, vol. 21, 2000.
[16] a. W. Gnauck A.H., P.J., " "Tutorial on Phase-Shift-Keyed Transmission"," presented at OFC 2004, 2004.
[17] S. E. Miller, *"Optical Fiber Communication 2";*: Academic Press, 1988.
[18] C. Wree, " "Experimental Investigation of receiver sensitivity of RZ-DQPSK modulation format using balanced detection";," presented at OFC2003, 2003.
[19] P. E. Green, *"Fiber Optic Networks"*: Prentice Hall, 1993.
[20] J. G. Proakis, *Digital Communications*, 3rd ed. New York: McGraw-Hill, 1995.
[21] J. C. Palais, *"Fiber Optic Communications"*: Prentic Hall, 1984.
[22] J. Armstrong, ""Simulink Optical Simulator"," in *Electrical and Computer Systems Engineering*. Clayton, Australia: Monash, 2003, pp. 62.
[23] A. Carera, " 'A time domain optical transmission system simulation package accounting for Nonlinear and Polarization-related effects in fiber' I.," *IEEE J. Selected Areas in Communications*, vol. 15, 1997.
[24] A. E. Elrefaie, " 'Chromatic Dispersion limitations in coherent lightwave transmission systems'," *IEEE J. Lightwave Technology*, vol. 6, 1988.
[25] G. P. Agrawal *Fiber-optic Communication Systems*, 2nd ed. N.Y.: Academic Press, 2002.
[26] G. Keiser, *"Optical Fiber Communication*. New York: McGraw Hill, 1991.
[27] X. Wei, " 'Numerical Simulation of the SPM penalty in a 10Gb/s RZ-DPSK system'," *IEEE Photonics technology Letters*, vol. 15, 2003.
[28] L. N. Binh, *"Optical Receiver: Noise and Sensitivity considerations for OFCS and networks"*. Melbourne Australia: MiTec, 2003.

8 Appendix:

8.1 Single channel DQPSK OFC system initialization Matlab m-file :

initialise_optical_simulator_DQPSK.m

```
%%%%%%%%%%%%%%%%%%%%%%%%%%%%%%%%%%%%%%%%%%%%%%%%%%%%%%%%%%%%%%
%%%%%%%%%%%%%%%%

%DQPSK Simulink Optical Simulator initialisation

%Written by Bernard Laville (13091948)

%Supervisor: Dr L N Binh

%Version 1.0, April 2004

%%%%%%%%%%%%%%%%%%%%%%%%%%%%%%%%%%%%%%%%%%%%%%%%%%%%%%%%%%%%%%
%%%%%%%%%%%%%%%%

%Note:

% Before running simulator define the standard system parameters

% then go to debug menu and select run, the DQPSK single channel simulink model

% will automatically open, press the run button in simulink to begin the simulation


% IMPORTANT: ENSURE THAT THE SCREENSAVER OPTION (CONTROL PANEL)IS TURNED OFF DURING

%           SIMULATION RUN-TIME. KEEP THE EYE DIAGRAM WINDOWS ON TOP

%           DURING SIMULATION RUN-TIME,

%           ALLOW SIMULATIONS TO CONCLUDE TO VIEW FULL EYE DIAGRAM

%%%%%%%%%%%%%%%%%%%%%%%%%%%%%%%%%%%%%%%%%%%%%%%%%%%%%%%%%%%%%%
%%%%%%%%%%%%%%%%


%standard system parameters
```

```
bitrate=10*10^9                   %bitrate in b/s

bitnum=256                        %number of bits in data string,

lambda=1550e-9                    %operating wavelength in m


%FIBER PARAMETERS (optional parameters varied for different fibers)

Dsmf=17e-6                        %SMF dispersion factor in s/m^2

Ddsf=3e-6                         %DSF dispersion factor in s/m^2

Ddcf=-85e-6                       %DCF dispersion factor in s/m^2

Lsmf=80000                        %SMF fiber length in m

Ldsf=80000                        %DSF fiber length in m

Ldcf=16000                        %DCF fiber length in m


speedlight=3*10^8                 %speed of light in m/s


%%%%%%%%%%%%%%%%%%%%%%%%%%%%%%%%%%%%%%%%%%%%%%%%%%%%%%%%%%%%%%%%%%%%%%%%%%%%%%%%%%%%%%
%system functions, no need to vary these values
%%%%%%%%%%%%%%%%%%%%%%%%%%%%%%%%%%%%%%%%%%%%%%%%%%%%%%%%%%%%%%%%%%%%%%%%%%%%%%%%%%%%%%


time=(bitnum-1)*(1/bitrate)       %simulation time for desired bit string


%%%%%%%%%%%%%%%%%%%%%%%%%%%%%%%%%%%%%%%%%%%%%%%%%%%%%%%%%%%%%%
%Photodiode Parameters
%%%%%%%%%%%%%%%%%%%%%%%%%%%%%%%%%%%%%%%%%%%%%%%%%%%%%%%%%%%%%%
```

```
R = 0.5  %Responsivity (1550nm) From Discovery Semiconductors Inc- DSC 10H Data Sheet

DarkI = 25 %Dark current in nm

Pmax = 20 %Maximum power rating in mW


%Inverted Cos-like photodiode current pulse approximation

t = 0:pi/10:2*pi;

Ipulse = -0.5*cos(t)+0.5;

open('C:\Report\BL_Simu_DQPSK\SingChanDQPSK_sim.mdl')

%open simulator model in simulink, may need to alter path if not on

%installation disk

%%%%%%%%%%%%%%end                                                    initialisation

file%%%%%%%%%%%%%%%%%%%%%%%%%%%%
```

8.2 Amplifier datasheet

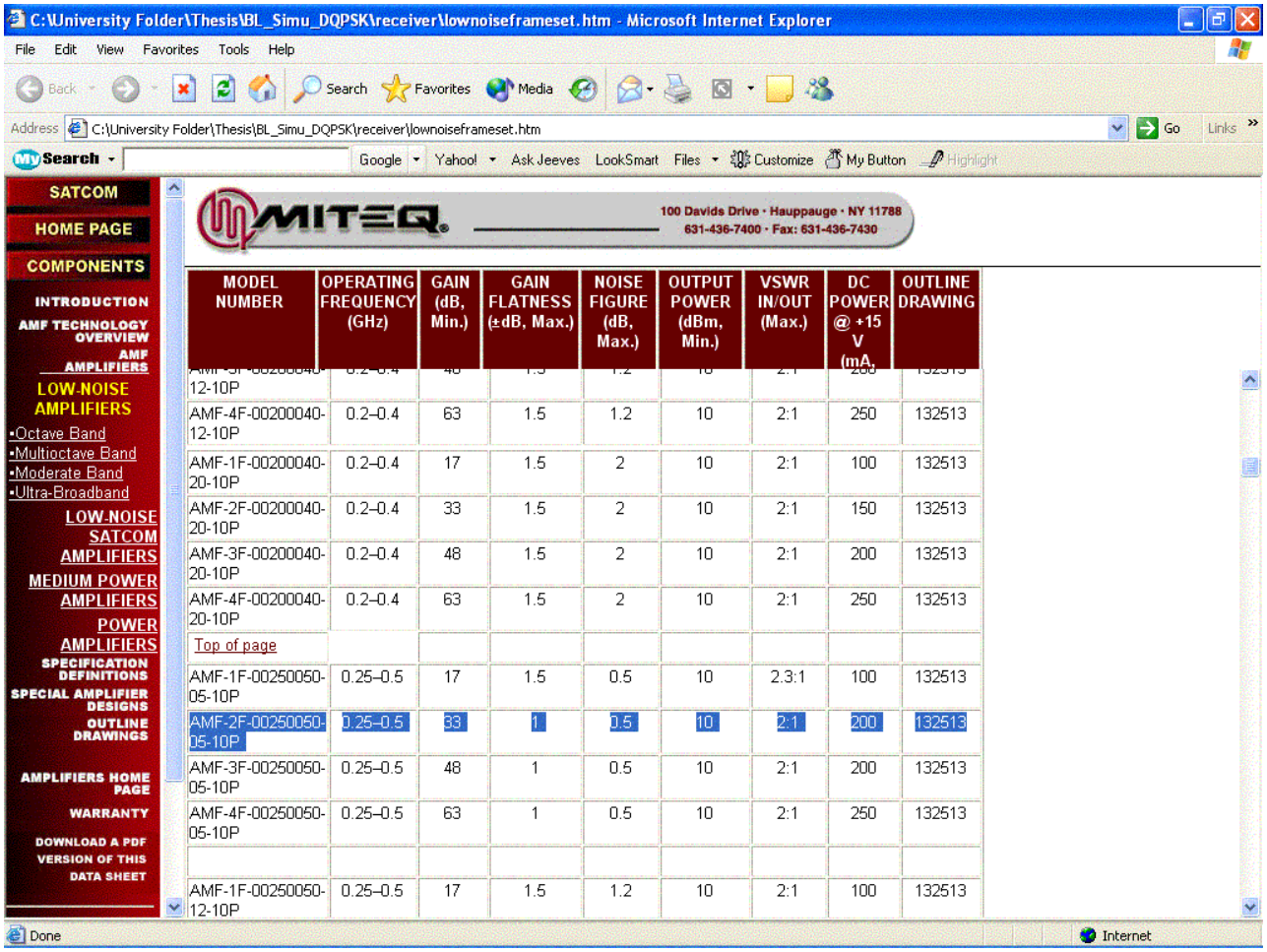

C:\University Folder\Thesis\BL_Simu_DQPSK\receiver\lownoiseframeset.htm - Microsoft Internet Explorer

File Edit View Favorites Tools Help

Back Search Favorites Media

Address C:\University Folder\Thesis\BL_Simu_DQPSK\receiver\lownoiseframeset.htm Go Links

MySearch Google Yahoo! Ask Jeeves LookSmart Files Customize My Button Highlight

SATCOM
HOME PAGE
COMPONENTS
INTRODUCTION
AMF TECHNOLOGY OVERVIEW
AMF AMPLIFIERS
LOW-NOISE AMPLIFIERS
•Octave Band
•Multioctave Band
•Moderate Band
•Ultra-Broadband
LOW-NOISE SATCOM AMPLIFIERS
MEDIUM POWER AMPLIFIERS
POWER AMPLIFIERS
SPECIFICATION DEFINITIONS
SPECIAL AMPLIFIER DESIGNS
OUTLINE DRAWINGS
AMPLIFIERS HOME PAGE
WARRANTY
DOWNLOAD A PDF VERSION OF THIS DATA SHEET

MITEQ 100 Davids Drive • Hauppauge • NY 11788 631-436-7400 • Fax: 631-436-7430

MODEL NUMBER	OPERATING FREQUENCY (GHz)	GAIN (dB, Min.)	GAIN FLATNESS (±dB, Max.)	NOISE FIGURE (dB, Max.)	OUTPUT POWER (dBm, Min.)	VSWR IN/OUT (Max.)	DC POWER @ +15 V (mA,	OUTLINE DRAWING
12-10P								
AMF-4F-00200040-12-10P	0.2–0.4	63	1.5	1.2	10	2:1	250	132513
AMF-1F-00200040-20-10P	0.2–0.4	17	1.5	2	10	2:1	100	132513
AMF-2F-00200040-20-10P	0.2–0.4	33	1.5	2	10	2:1	150	132513
AMF-3F-00200040-20-10P	0.2–0.4	48	1.5	2	10	2:1	200	132513
AMF-4F-00200040-20-10P	0.2–0.4	63	1.5	2	10	2:1	250	132513
Top of page								
AMF-1F-00250050-05-10P	0.25–0.5	17	1.5	0.5	10	2.3:1	100	132513
AMF-2F-00250050-05-10P	0.25–0.5	33	1	0.5	10	2:1	200	132513
AMF-3F-00250050-05-10P	0.25–0.5	48	1	0.5	10	2:1	200	132513
AMF-4F-00250050-05-10P	0.25–0.5	63	1	0.5	10	2:1	250	132513
AMF-1F-00250050-12-10P	0.25–0.5	17	1.5	1.2	10	2:1	100	132513

Done Internet